Phyllosphere exudates select for distinct microbiome members in sorghum epicuticular wax and aerial root mucilage

Marco E. Mechan-Llontop[1,2], John Mullet[2,3], and Ashley Shade[1,2,4,5,6*]

[1]Department of Microbiology and Molecular Genetics, Michigan State University, East Lansing, MI, 48824.

[2]Great Lakes Bioenergy Research Center, Michigan State University, East Lansing, MI, 48824.

[3]Department of Biochemistry & Biophysics, Texas A&M University, College Station, TX, 77843

[4]Department of Plant, Soil and Microbial Sciences, Michigan State University, East Lansing MI 48824

[5]The Plant Resilience Institute, Michigan State University, East Lansing MI 48824

[6] Univ Lyon, CNRS, INSA Lyon, Université Claude Bernard Lyon 1, École Centrale de Lyon, Ampère, UMR5005, 69134, Ecully cedex, France. *(Present address)*

*Corresponding author: A. Shade; E-mail: ashley.shade@cnrs.fr

ABSTRACT

Phyllosphere exudates create specialized microhabitats that shape microbial community diversity. We explored the microbiome associated with two sorghum phyllosphere exudates, the epicuticular wax and aerial root mucilage. We assessed the microbiome associated with the wax from sorghum plants over two growth stages, and the root mucilage additionally from nitrogen-fertilized and non-fertilized plants. In parallel, we isolated and characterized hundreds of bacteria from wax and mucilage, and integrated data from cultivation-independent and cultivation-dependent approaches to gain insights into exudate diversity and bacterial phenotypes. We found that *Sphingomonadaceae* and *Rhizobiaceae* families were the major taxa in the wax regardless of water availability and plant developmental stage to plants. The cultivation-independent mucilage-associated bacterial microbiome contained *Erwiniaceae, Flavobacteriaceae, Rhizobiaceae, Pseudomonadaceae, Sphingomonadaceae*, and its structure was strongly influenced by sorghum development but only modestly influenced by fertilization. In contrast, the fungal community structure of mucilage was strongly affected by the year of sampling but not by fertilization or plant developmental stage, suggesting a decoupling of fungal-bacterial dynamics in the mucilage. Our bacterial isolate collection from wax and mucilage had several isolates that matched 100% to detected amplicon sequence variants, and were enriched on media that selected for phenotypes including phosphate solubilization, putative diazotrophy, resistance to desiccation, capability to grow on methanol as a carbon source, and ability to grow in the presence of linalool and β-caryophyllene (terpenes in sorghum wax). This work expands our understanding of the microbiome of

phyllosphere exudates and supports our long-term goal to translate microbiome research to support sorghum cultivation.

Keywords: bioenergy, agriculture microbiome, bacterial isolates, plant-association, diazotroph, irrigation, fertilizer, amplicon sequencing, cultivation

INTRODUCTION

The phyllosphere, which includes the above-ground plant structures, has diverse surface features (Ruinen 1965; Vacher et al. 2016; Doan et al. 2020). It is a microbial habitat that is exposed to rapid environmental fluctuations and stressors, including in ultraviolet radiation, temperature, and nutrient and water availability. Thus, the diversity and functions of the phyllosphere microbiome reflects this complex habitat (Lindow and Brandl 2003; Vorholt 2012; Vacher et al. 2016). To adapt to abiotic stresses, plants produce a diversity of exudates on their external surfaces (Chai and Schachtman 2022). The secreted exudates vary in composition and structure, creating specialized phyllosphere microhabitats (Galloway et al. 2020). Exudates that accumulate in the phyllosphere include epicuticular wax on stems and leaves (Kunst and Samuels 2003), sugar-rich mucilage on aerial root structures (Bennett et al. 2020), floral nectaries (Rering et al. 2018), and extrafloral nectaries in stems and leaves (Pierce 2019). Because of their potential as locations of microbial engagement with the host, research has been initiated to explore these microbial communities that reside on phyllosphere exudates.

Plants secrete epicuticular wax on leaves, leaf sheaths, and stems for prevention of water loss under drought stress (Xue et al. 2017), reflection of solar radiation (Steinmüller and Tevini 1985), and pathogen protection (Serrano et al. 2014; Wang et al. 2020). Epicuticular waxes are enriched in long-chain hydrocarbons. The major wax components include alkanes, alcohols, esters, and fatty acids, as well as varying levels of triterpenoids, sterols, and flavonoids (von Wettstein-Knowles 1974; Kunst and Samuels 2003; Busta et al. 2021). The wax composition and quantities are affected by plant species, plant developmental stage, and environmental conditions (Yeats and Rose 2013). It has been shown that epicuticular waxes affect bacterial and fungal plant colonization in a species-dependent manner (Beattie and Marcell 2002; Tsuba et al. 2002). Also, wax accumulation and composition directly impact the phyllosphere microbial community diversity (Reisberg et al. 2013). A study in *Arabidopsis thaliana* reported that Proteobacteria, Bacteroidetes, and Actinobacteria were the dominant phyla associated with wax on leaves (Reisberg et al. 2013).

Plants also secrete an abundance of polysaccharide-rich mucilage on aerial roots and the above ground portion of brace roots. Brace roots support plant anchorage as well as water and nutrient uptake (Stamp and Kiel 1992; Ku et al. 2012; Reneau et al. 2020). In 2018, van Deynze et al. 2018 reported that the mucilage of aerial roots of a maize landrace harbored diazotrophic microbiota that provided almost 80% of the nitrogen needed by the host. The bacterial genera *Acinetobacter*, *Agrobacterium*, *Enterobacter*, *Klebsiella*, *Lactococcus*, *Pantoea*, *Pseudomonas*, *Rahnella*, *Raoultella*, *Stenotrophomonas*, and others have been found in association with the mucilage of

maize. These bacteria were capable of biological nitrogen fixation (BNF), synthesizing indole-3-Acetic Acid (IAA), utilizing 1-amino-1-cyclopropanecarboxylic acid (ACC), and solubilizing phosphates. The unique polysaccharide composition of the mucilage may modulate its associated microbiota (van Deynze et al. 2018; Higdon et al. 2020b). The maize mucilage is enriched in a mixture of monosaccharides including fucose (28%), galactose (22%), arabinose (15%), glucuronic acid (11%), xylose (11%), mannose (8%), glucose (1%) and galacturonic acid (1%) (van Deynze et al. 2018; Amicucci et al. 2019). The polysaccharide composition of root mucilage may vary among maize genotypes and with changing environmental conditions (Nazari et al. 2020).

Bioenergy sorghum (*Sorghum bicolor* L. Moench) is a heat and drought-tolerant annual crop being developed for production of biomass, biofuels and bioproducts (Mullet et al. 2014; Varoquaux et al. 2019). Bioenergy sorghum confers 75%-90% greenhouse gas mitigation when used for ethanol production or biopower generation respectively (Olson et al. 2012), but excess nitrogen fertilizer is required to grow it, resulting in the release of nitrous oxide and relatively lower carbon benefit than other biofuel feedstocks that do not have high fertilizer demands (Kent et al. 2020; Scully et al. 2021). In the 1980s, it was hypothesized that the mucilage secreted by sorghum aerial roots harbors diazotroph bacteria, as has been more recently shown in the a maize landrace (Bennett et al. 2020), but this has not yet been experimentally confirmed. Although the polysaccharide composition of the sorghum aerial root mucilage is uncharacterized, it is expected that the sorghum mucilage is similar in composition to maize (van Deynze et al. 2018; Amicucci et al. 2019). Taken together, it

is expected that understanding microbiome interactions on the sorghum mucilage may provide insights into microbiome-enabled solutions to optimize diazotrophic nitrogen for the host and, in parallel, reduce nitrogen fertilizer needs for bioenergy sorghum.

Like other plants, bioenergy sorghum accumulates high levels of epicuticular wax on stems and leaves over its development, and some functions of the wax are to exclude pathogens and prevent water loss. Sorghum epicuticular wax chemistry and structure have been extensively studied. The accumulation, and composition of sorghum epicuticular wax are affected by several factors, including plant age, genotype, water availability, and environmental stresses (Bianchi et al. 1978; Avato et al. 1984; Jordan et al. 1984; Steinmüller and Tevini 1985; Shepherd et al. 1995; Jenks et al. 1996; Bondada et al. 1996; Shepherd and Wynne Griffiths 2006; Xue et al. 2017). However, the influence of sorghum wax chemistry on bacteria colonization and community structure is unknown.

In the present study, we investigated the microbiome associated with bioenergy sorghum epicuticular wax and aerial root mucilage. Given the functions of these exudates for the host, these communities may be of interest to examine microbiome traits that support host drought tolerance and nutrient uptake. To begin to explore the microbial communities inhabiting these specialized phyllosphere exudates, the microbiome composition and structure of wax and mucilage was analyzed from field conditions that included management treatments expected to influence plant water and nitrogen status. Specifically, we assessed the bacterial microbiome associated with the epicuticular wax from sorghum plants at two different developmental stages that also

131 received different amounts of water, and the bacterial and fungal microbiomes
132 additionally associated with the aerial root mucilage from nitrogen (N)-fertilized and non-
133 fertilized sorghum plants. In addition, we curated a bacterial isolate collection from each
134 phyllosphere exudate. We integrate data from both cultivation-independent and -
135 dependent approaches to gain deeper insights into the microbiome diversity and
136 dynamics of sorghum epicuticular wax and aerial root mucilage.

137 We hypothesized that: 1) wax and mucilage harbor different bacterial
138 microbiomes due to their different exudate chemistries, host functions, and
139 compartments; 2) plant developmental stage and watering status has highest
140 explanatory value for the wax bacterial microbiota due to the known role of wax in
141 supporting plant drought tolerance; 3) fertilization status has highest explanatory value
142 for the mucilage bacterial microbiota due to changes in exogenous nutrient availability
143 that are expected to result in changes in mucilage polysaccharide composition; and 4)
144 that the bacterial and fungal members of the mucilage microbiome exhibit similar
145 dynamics due to expected similar host and environmental drivers.

146

147 **METHODS**

148

149 **Collection of sorghum stems and recovery of epicuticular wax**. We collected
150 samples from the bioenergy sorghum *(Sorghum bicolor)* hybrid TX08001 grown at the
151 Texas A&M University Research Farm in College Station, Texas (30°55'5.55" N,
152 96°.43'64.6" W). Sorghum plants were grown in 5 replicate 32 rows by 30 m plots at

153 standard planting density and fertilization (Olson et al., 2012). We sampled replicate
154 plots 1-5 at 60 (08/03/2020) and 90 (09/02/2020) days after plant emergence (DAE).
155 While sorghum plants at 60 DAE were irrigated to maintain non-limiting water status,
156 plants at 90 DAE were grown without irrigation to induce water-limiting conditions until
157 harvesting. Thus, the developmental age of the plants and their watering status are
158 colinear and their effects cannot be separated in our study. We collected stem sections
159 that were covered in epicuticular wax, using razor blades to destructively sample the
160 fifth and sixth fully elongated stem node-internodes below the growing zone into sterile
161 whirl-pak bags. In total, we collected 50 stem samples during the growing season of
162 2020. All samples were kept on ice for transport, shipped on dry ice to Michigan State
163 University, and then stored at -80 °C. We used sterile razor blades to carefully remove
164 and collect the epicuticular wax from stems in sterile 1.5 ml Eppendorf tubes.
165 Epicuticular wax samples were stored at -80 °C until processing.
166
167 C**ollection of sorghum aerial roots and removal of the mucilage**. We collected
168 samples from the bioenergy sorghum cultivar TAM 17651 grown at the Great Lakes
169 Bioenergy Research Center (GLBRC), as part of the Biofuel Cropping System
170 Experiment (BCSE) in Hickory Corners, Michigan (42°23'41.6" N, 85°22'23.1" W).
171 Sorghum plants were grown in 5 replicate 30x40 m plots arrayed in a randomized
172 complete block design. Within each plot, nitrogen fertilizer-free subplots were
173 maintained either in the western or eastern -most 3m of each plot. We sampled
174 replicate plots 1-4 in both the main and nitrogen-fertilizer free subplots at 60 and 90

DAE. We used sterile razor blades to carefully collect between 3 to 5 aerial nodal roots per plant that were covered with visible mucilage into sterile 50 ml Eppendorf tubes. In total, we collected 180 aerial root samples during the growing seasons of 2020 and 2021. All samples were kept on ice for transport, and then stored at -80 ^{o}C. In the laboratory, we added 15 ml of sterile distilled water and kept the roots for 5 min at room temperature to fully hydrate the aerial root mucilage. We collected 1 ml of mucilage into sterile 1.5 ml Eppendorf tubes per sample. Mucilage samples were stored at -80 ^{o}C until processing.

Culturing the epicuticular wax and mucilage microbiomes. For bacterial isolation, we pooled the epicuticular wax collected from different plants, as described above, and resuspended 100 mg of wax in 1 ml of sterile distilled water. We also pooled the mucilage collected from different plants, as described above. To capture a diversity of bacteria from the wax and mucilage, we used a variety of cultivation media (**Table 1**). First, we used standard culture media with a relatively high concentration of nutrients, including Tryptic Soy Agar (TSA: casein peptone 15 gl^{-1}, soy peptone 5 gl^{-1}, sodium chloride 5 gl^{-1}, agar 15 gl^{-1}, pH 7.3) and 50TSA (1/2 dilution of TSA). We also used media with relatively lower concentrations of nutrients, including Reasoner's 2A (R2A: yeast extract 0.5 gl^{-1}, proteose peptone N^{o}3 0.5 gl^{-1}, casamino acids 0.5 gl^{-1}, glucose 0.5 gl^{-1}, soluble starch 0.5 gl^{-1}, sodium pyruvate 0.3 gl^{-1}, K_2HPO_4 0.3 gl^{-1}, $MgSO_4$ x $7H_2O$ 0.05 gl^{-1}, agar 15 gl^{-1}), 50R2A (1/2 dilution of R2A), and M9 minimal media (Na_2HPO_4 12.8 gl^{-1}, KH_2PO_4 3.0 gl^{-1}, NaCl 0.5 gl^{-1}, NH_4Cl 1.0 gl^{-1}, glucose 20 gl^{-1}, 1M $MgSO_4$

197 solution 20 ml, 1M $CaCl_2$ solution 0.1 ml, thiamine 0.5% w/v solution 0.1 ml, agar 15 gl^{-1}).
198 To enrich for bacteria with putative plant beneficial traits, we used selective media
199 types, including Jensen's medium (sucrose 20 gl^{-1}, K_2HPO_4 1 gl^{-1}, $MgSO_4$ 0.5 gl^{-1}, NaCl
200 0.5 gl^{-1}, $FeSO_4$ 0.1 gl^{-1}, Na_2MoO_4 0.005 gl^{-1}, $CaCO_3$ 2 gl^{-1}, agar 1 gl^{-1}) and modified
201 nitrogen-free M9 minimal media with and without 1% (w/v) D-arabinose, galactose or
202 xylose at pH 5, 5.8 or 7 (Na_2HPO_4 12.8 gl^{-1}, KH_2PO_4 3.0 gl^{-1}, NaCl 0.5 gl^{-1}, 1M $MgSO_4$
203 solution 20 ml, 1M $CaCl_2$ solution 0.1 ml, agar 15 gl^{-1}) for detection of putative nitrogen
204 fixing bacteria, Pirovskaya's agar (yeast extract 0.5 gl^{-1}, dextrose 10 gl^{-1}, $Ca_3(PO_4)_2$ 5 gl^{-1}),
205 $(NH_4)_2SO_4$ 0.5 gl^{-1}, KCl 0.2 gl^{-1}, $MgSO_4$ 0.1 gl^{-1}, $MnSO_4$ 0.0001 gl^{-1}, $FeSO_4$ 0.0001 gl^{-1},
206 agar 15 gl^{-1}) for detection of phosphate solubilizing bacteria, Gauze's synthetic medium
207 Nº1 (soluble starch 20 gl^{-1}, KNO_3 1 gl^{-1}, NaCl 0.5 gl^{-1}, $MgSO_4$ x $7H_2O$ 0.5 gl^{-1}, K_2HPO_4
208 0.5 gl^{-1}, $FeSO_4$ x 7 H_2O 10 mgl^{-1}, agar 15 gl^{-1}) for isolation of Actinobacteria, King's
209 medium B (proteose peptone 20 gl^{-1}, K_2HPO_4 1.5 gl^{-1}, $MgSO_4$ x $7H_2O$ 1.5 gl^{-1}, glycerol
210 10 ml) for isolation of fluorescent pseudomonas, and methanol mineral salts medium
211 ($(NH_4)_2SO_4$ 2.0 gl^{-1}, NH_4Cl 2.0 gl^{-1}, $(NH_4)_2HPO_4$ 2.0 gl^{-1}, KH_2PO_4 1.0 gl^{-1}, K_2HPO_4 1.0 gl^{-1},
212 $MgSO_4$ x $7H_2O$ 0.5 gl^{-1}, Fe_2SO_4 x $7H_2O$ 0.01 gl^{-1} ,$CaCl_2$ x $2H_2O$ 0.01 gl^{-1}, yeast extract
213 2.0 gl^{-1}, agar 20 gl^{-1}) for isolation of methanol-utilizing bacteria.

214 All plates were incubated for up to 14 days. To select for anaerobic bacteria, agar
215 plates were placed in anaerobic jars (Mitsubishi AnaeroPack 7.0L rectangular jar)
216 containing three bags of anaerobic gas generator (Thermo Scientific AnaeroPack
217 Anaerobic Gas generator). To enrich for bacteria resistant to desiccation, one hundred
218 microliters of dilution 10^{-1} from the wax and mucilage were inoculated on 20 ml of 50%

TSB liquid culture supplemented with different concentrations of 6000 polyethylene-glycol, including –0.49 MPa (210 gl^{-1} PEG w/v), -0.73 MPa (260 gl^{-1} PEG w/v) and –1.2 MPa (326 gl^{-1} PEG w/v). To enrich for bacteria that can grow in the presence of terpenoids, 100 ml of dilution 10^{-1} from the wax and mucilage were inoculated on 20 ml of 50% TSB liquid culture supplemented with 1% (v/v) of either linalool or β-caryophyllene. Liquid cultures were incubated at 28°C for 24 h, and dilutions 10^{-1} to 10^{-4} were plated in duplicate on R2A agar plates for 24 h. Well isolated individual colonies were picked with a sterile toothpick and transferred to a new R2A plate. To confirm bacterial purity, individual bacterial colonies were transferred three times on new R2A agar plates. Glycerol stock (25% v/v) of pure bacteria isolates were stored at -80°C.

Metagenomic DNA extraction and amplicon sequencing. Microbial DNA was extracted from 0.5 ml of mucilage and 100 mg of epicuticular wax using a DNeasy PowerSoil kit (Qiagen, Maryland, USA) according to the manufacturer's instructions. To confirm successful DNA extraction, the metagenomic DNA was quantified using a qubit 2.0 fluorometer (Invitrogen, Carlsbad, CA, USA), and visualized in a 1% agarose gel. Then, the PCR amplifications and sequencing of the V4 region of the 16S rRNA bacterial or archaeal gene from the epicuticular wax and mucilage samples and the ITS1 region of the fungal rRNA gene from the mucilage samples only were performed. DNA concentrations were normalized to approximately 1 $\mu g/\mu l$ between all samples before PCR amplification and sequencing. The V4 hypervariable region of the 16S rRNA gene was amplified using the universal primers 515F (5′-

GTGCCAGCMGCCGCGGTAA- 3′) and 806R (5′-GGACTACHVGGGTWTCTAAT-3′) (Caporaso et al. 2011) under the following conditions: 95°C for 3 min, followed by 30 cycles of 95°C for 45 s, 50°C for 60 s, and 72°C for 90 s, with a final extension at 72°C for 10 min. The metagenomic DNA of each sample was submitted to the Genomics Core of the Research Technology Support Facility at Michigan State University for library preparation and sequencing using the Illumina MiSeq platform v2 Standard flow cell in a 2x250bp paired-end format, using their standard operating protocol.

The ITS1 region was amplified using primers ITS1f (5′-CTTGGTCATTTAGAGGAAGTAA-3′) and ITS2 (5′-GCTGCGTTCTTCATCGATGC-3′) (Smith and Peay 2014) with the addition of index adapters CS1-TS-F: 5' – ACACTGACGACATGGTTCTACA – [TS-For] – 3' and CS2-TS-R: 5' – TACGGTAGCAGAGACTTGGTCT – [TS-Rev] – 3' as requested by the Genomics Sequencing Core under the following PCR conditions: 94°C for 3 min, followed by 35 cycles of 94°C for 30 s, 52°C for 30 s, and 68°C for 30 s, with a final extension at 68°C for 10 min. The amplification was performed with GoTaq Green Master Mix (Promega). The PCR products were purified with ExoSAP-IT reagent, and sample sequencing was completed by the Genomics Core of the Research Technology Support Facility at Michigan State University using the Illumina MiSeq platform v2 Standard flow cell in a 2x250bp paired-end format. For quality control purposes, positive and negative controls were included throughout the DNA extraction, PCR amplification, and sequencing processes. A 75 μl aliquot of the ZymoBIOMICS Microbial Community

Standard (Zymo Research, Irvine, CA, U.S.A) and 75 μl aliquot of an in-house Community Standard were included as positive controls. Sterile DEPC-treated water was included as negative control.

Bacterial genomic DNA extraction. Bacteria colonies that were first streaked and isolated for purity were grown on 2 ml of 50% TSB liquid culture at 28°C for 24 h. Bacteria culture was centrifuged at 5,000 rpm for 10 min. Genomic DNA of each isolate was extracted by using the Zymo – Quick DNA Fungal/Bacterial 96 kit following the manufacturer's protocol. Total genomic DNA was quantified using a qubit 2.0 fluorometer and visualized in a 1% agarose gel. The PCR amplification of the full-length 16S rRNA gene with universal primers 27F (5′-AGAGTTTGATCCTGGCTCAG-3′) and 1492R (5′-TACGGTTACCTTGTTACGACTT-3′) (Miller et al. 2013) was performed by using the Pfu Turbo DNA polymerase (Agilent) under the following conditions: 95°C for 2 min, followed by 24 cycles of 95°C for 30 s, 48°C for 30 s, and 72°C for 3 min, with a final extension at 72°C for 10 min. PCR products were purified with ExoSAP-IT reagent and submitted for Sanger sequencing at the Genomics Core of the Research Technology Support Facility at Michigan State University, MI, USA.

Bacterial and fungal amplicon sequencing analysis. Paired-end sequencing data from each sequencing experiment were processed with QIIME2 (Bolyen et al. 2019) version 2021.8.0. In brief, sequences were imported using the PairedEndFastqManifestPhred33V2 format. Sequence quality control, denoising, and

generation of feature tables containing counts for the Amplicon Sequencing Variants (ASVs) were performed with the q2-dada2 plugin version 2021.8.0 (Callahan et al. 2016). Trimming parameters for the DADA2 plugin were selected with FIGARO version 1.1.2 (Weinstein et al. 2019). ASVs tables and representative sequences from each sequencing experiment were merged with the q2-feature-table plugin. ASV taxonomy (of merged ASVs) was assigned with the q2-feature-classifier plugin using the SILVA version 1.38 database (Quast et al. 2013) for bacteria and UNITE version 8.3 database (Nilsson et al. 2019) for fungi.

The ASV table, taxonomy table, and sample metadata files were imported into R version 4.1.3 for data visualization and statistical analysis. Diversity and statistical analyses were performed using the phyloseq (McMurdie and Holmes 2013) and vegan (Dixon 2003) packages. Treatments compared were: exudate (wax, mucilage) for bacterial microbiomes; fertilization status (fertilized, unfertilized), year of sample collection (2020, 2021), and developmental stage (60 DAE, 90 DAE) for mucilage bacterial and fungal microbiomes; and developmental stage/water availability (60 DAE, 90 DAE) for wax bacterial microbiomes. A Wilcoxon rank sum test with continuity correction was used to test for differences in alpha diversity across treatments. Permuted analysis of variance (PERMANOVA) and permuted analysis of beta-dispersion (PERMDISP) were used to assess differences in beta diversity structure across treatments by centroid and dispersion. Differential abundance analysis was performed with the DESeq2 package (Love et al. 2014). Each dataset (bacterial/fungal, wax/mucilage) was subsampled independently to ensure maximum coverage for

comparisons over time and across field treatments. The exception was when testing hypothesis 1 (differences in wax and mucilage bacterial microbiome), and in this case both datasets were subsampled to an even 2,500 sequences per sample for comparison.

Full-length 16S rRNA gene Sanger sequencing analysis: Culturing phyllosphere exudate microbiota. To generate a consensus sequence of the full-length 16S rRNA gene from each bacterial isolate, sequences were imported into Geneious version 2021.2.2 (https://www.geneious.com/). High-quality forward and reverse sequences were aligned and trimmed to generate a consensus sequence. Then, the consensus sequence was searched with BLAST for taxonomic classification. CD-HIT version 4.8.1 (Li and Godzik 2006) was used to remove redundant 16S rRNA sequences. To identify bacterial isolates that match 100% to the identified ASVs from the culture-independent approach, a local BLAST search was performed. In summary, a local BLAST database was created with all non-redundant 16S rRNA sequences from our bacterial collection using the *makeblastdb* command and the *-dbtype nucl* option. A BLAST search was carried out to identify related sequences in the representative sequences (ASVs dna-sequences.fasta) file generated from the DADA2 denoising step with the *blastn* command, and the flowing options: "6 qseqid sseqid pident length mismatch gapopen qstart qend sstart send evalue bitscore".

328 **Comparison with publicly available plant-associated bacterial genomes.** We
329 retrieved 637 plant-associated (PA) bacterial genomes that were classified as non-root
330 associated from the (Levy et al. 2017) study. High-quality bacterial genomes were
331 annotated with Prokka (Seemann 2014) using an in-house python script and annotated
332 16S rRNA gene copies were identified (available on GituHub, see Data availability
333 statement). For bacteria with multiple 16S rRNA copies, CD-HIT version 4.8.1 (Li and
334 Godzik 2006) was used to remove redundant sequences (99% similarity) and one 16S
335 rRNA sequence was conserved, totaling 433 unique PA sequences. All 16S rRNA
336 sequences from the PA bacterial genome dataset were concatenated in a single fasta
337 file with the *cat* command. CD-HIT was used to remove redundant sequences (100 %
338 similarity) from the 16S rRNA concatenated file. All non-redundant 16S rRNA
339 sequences from both the sorghum bacterial collections and the publicly available PA
340 bacteria were merged in a single *fasta* file. Sequence alignment was performed with
341 MAFFT v7.407 (Katoh et al. 2002). Alignment trimming was performed with trimAl
342 (Capella-Gutiérrez et al. 2009). A maximum-likelihood (ML)-based phylogenetic tree
343 was built with IQ-TREE 2.2.0-beta version (Minh et al. 2020). ModelFinder version (-m
344 TEST option) (Kalyaanamoorthy et al. 2017) was used to select the best model for the
345 phylogenetic tree construction. Branch support was assessed using 1,000 ultrafast
346 boostrap approximations (-bb 1000 option) (Hoang et al. 2018). Phylogenetic diversities
347 were calculated as the total tree length, that represents the expected number of
348 substitutions per site. Phylogenetic tree was edited with iTOLs version 6.5.8 (Letunic
349 and Bork 2021).

Data and code availability. The data analysis workflows for sequence processing and ecological statistics are available on GitHub (https://github.com/ShadeLab/Sorghum_phyllosphere_microbiome_MechanLlontop_2022.git). Raw sequencing data has been deposited in the Sequence Read Archive NCBI database under BioProject accession number PRJNA844896 (including 16S rRNA and ITS amplicons). Full-length 16S rRNA sequence data has been deposited in the GenBank with accession numbers ON973084-ON973283.

RESULTS

Sequencing summary. In total, we sequenced the bacterial 16S rRNA V4 region from 48 epicuticular wax samples from the 2020 growing season, as well as the bacterial 16S rRNA V4 region from 179 mucilage samples and the fungal ITS region from 173 mucilage samples that were collected across two growing seasons in 2020 and 2021. We obtained 8,648,839 bacterial sequences from the wax, and 20,606,039 bacterial and 20,181,404 fungal sequences from the mucilage. After quality control, removal of chimeras, and denoising, 7,930,768 quality bacterial reads were obtained from the wax samples, and 19,880,634 bacterial and 12,157,819 fungal sequences were obtained from mucilage **(Table 2)**. For wax, the total number of sequences per sample after the denoising process with DADA2 into Amplicon Sequence Variants (ASVs) ranged from 1,722 to 272,108. After the removal of nonbacterial and unassigned sequences, a total of 2,386,033 sequences remained, with sequencing reads per wax sample ranging from

138 to 206,128. We removed wax samples with fewer than 1000 sequences, and the remaining 42 epicuticular wax samples were rarefied to 1,303 sequences for further analysis **(Figure 1A)**. Given the observed richness (12 to 93 ASVs per sample) by these cultivation-independent methods, Figure 1A shows that the wax bacterial microbiome was covered with the given sequencing effort.

For root mucilage, the number of bacterial sequences per sample after the denoising ranged from 222 to 330,853. After the removal of nonbacterial and unassigned sequences, a total of 12,956,774 sequences remained, with sequencing reads per sample ranging from 110 to 235,069. We removed samples with fewer than 20,000 sequences, and the remaining 158 samples were rarefied to 20,519 sequences for comparative analysis **(Figure 1B)**. Given the observed richness (49 to 555 ASVs per sample) by these cultivation-independent methods, Figure 1B shows that the mucilage bacterial microbiome was covered with the given sequencing effort. The number of fungal sequences per mucilage sample after the denoising ranged from 78 to 119,207. After the removal of non-fungal and unassigned sequences, a total of 12,297,453 sequences remained, with sequencing reads per sample ranging from 32 to 119,207. We filtered mucilage samples with fewer than 30,000 ITS sequences, and the remaining 171 samples were rarefied to 33,975 sequences for comparative analysis **(Figure 1C)**. Similarly, given the observed richness by these cultivation-independent methods (47 to 237 ASVs per sample), **Figure 1C** shows that the mucilage fungal microbiome was covered with the given sequencing effort.

Hypothesis 1: Wax and mucilage harbor different bacterial microbiomes

Compositional differences in the bacterial microbiomes of the epicuticular wax and mucilage were apparent at the family level of taxonomic resolution (**Figure 2A and B)** as well as at the genus level **(Supplementary Figure S1A and B**). Wax and mucilage bacterial microbiomes had different richness (observed taxa Wilcoxon rank $p<0.001$, **Supplementary Table 1**) and different structures (PERMANOVA R-squared= 0.14, $p=0.001$). Thus, Hypothesis 1 was supported. However, there were no differences detected in the dispersions of wax and mucilage bacterial microbiome structures (PERMDISP F=0.69, $p=0.43$).

Hypothesis 2: Plant developmental stage/watering status has highest explanatory value for the wax bacterial microbiota

Altogether, we identified 534 bacterial ASVs in epicuticular wax. Wax bacterial microbiome samples collected from sorghum plants at 60 DAE and 90 DAE had different richness (observed taxa Wilcoxon rank $p= 0.03$) **(Supplementary Table 1)**. There was higher variation in the community structure in the epicuticular wax on plants at 90 DAE compared with plants at 60 DAE (PERMDISP F=17.92, $p=0.001$). There was a small but significant influence of sorghum developmental stage on the epicuticular wax community structure **(**PERMANOVA R-squared=0.06, $p= 0.003$, **Figure 3A**, **Table 3)**.

The sorghum epicuticular wax microbiome was dominated by the Proteobacteria (84% mean relative abundance) and Bacteroidetes (11%) bacteria phyla. The bacterial

416 classes Alphaproteobacteria (54%), Gammaproteobacteria (30%), and Bacteroidia
417 (11%) were in highest abundance. Sphingomonadaceae (25%), Rhizobiaceae (21%),
418 and Xanthomonadaceae (7%) were the major bacterial families in sorghum epicuticular
419 wax **(Figure 2A).** At the genus level, *Sphingomonas* (28%), *Rhizobium* (12%),
420 *Aureimonas* (10%), and *Acinetobacter* (5%) were the dominant taxa in wax
421 **(Supplementary Figure 1)**. Differential abundance analysis showed that only one ASV
422 (ASV ID #5438e75153393c2dda98fe3d99c26da1) from the Microbacteriacea family was
423 more abundant on the wax of plants at 60 DAE (by 3.08-fold, DeSeq $p = 0.01$), and that
424 one ASV (ASV ID #8f820a46cfecd19477f4485d1c436764) assigned to
425 *Pseudoxanthomonas* genera was more abundant on the wax of plants at 90 DAE (by
426 4.49-fold, DESeq $p = 0.01$). Taking these results together, Hypothesis 2 was weakly
427 supported with a small, significant difference in wax bacterial microbiome by plant stage
428 and two taxa that were distinguishing between the stages.
429
430 **Hypothesis 3: Fertilization status has highest explanatory value for the bacterial**
431 **mucilage microbiota**
432 Altogether, 12,047 bacterial ASVs were identified in aerial root mucilage. There was no
433 difference in richness between mucilage samples collected from sorghum plants at 60
434 DAE and 90 DAE (observed species Wilcoxon rank $p = 0.82$, **Supplementary Table 1**),
435 and also no difference between mucilage samples from nitrogen-fertilized plants as
436 compared with unfertilized plants. **(**observed species Wilcoxon rank $p = 0.15$,
437 **Supplementary Table 1)**. There was different beta dispersion in community structure

by plant developmental stage (PERMDISP F=19.56, p=0.001) but not by fertilization status (PERMDISP F=1.83, p=0.187). The mucilage bacterial microbiome structure was better explained by developmental stage than fertilization status (PERMANOVA R-squared= 0.14 and 0.03, respectively, both p= 0.001) **(Figure 3B).**

The aerial root mucilage bacterial microbiome was dominated by the Proteobacteria (61% mean relative abundance) and Bacteroidota (36%) bacteria phyla. The bacterial class Gammaproteobacteria (40%), Bacteroidia (34%), and Alphaproteobacterial (21%) were the most abundant. Erwiniaceae (23%), Rhizobiaceae (14%), Flavobacteriaceae (12%), Pseudomonadaceae (9%), and Sphingomonadaceae (6%) were the major bacterial families in mucilage (**Figure 2B)**. A differential abundance analysis identified 25 ASVs enriched in the mucilage at 60 DAE and 72 ASVs significantly enriched in plants at 90 DAE **(Figure 4,** DESeq p = 0.01). Taking these results together, Hypothesis 3 was not supported, and the bacterial microbiome of the mucilage was not highly sensitive in structure or dispersion to fertilization given this study's field conditions, nor were there notable distinguishing taxa by plant fertilization status.

Hypothesis 4: The bacterial and fungal members of the mucilage microbiome exhibit similar dynamics.

Altogether, 5,641 fungal ASVs were identified in aerial root mucilage. There were differences in richness between mucilage samples collected from sorghum plants during the 2020 and 2021 growing seasons (observed species Wilcoxon rank p = 0.008), and

also between mucilage samples from nitrogen-fertilized plants compared with unfertilized plants (observed species Wilcoxon rank $p < 0.01$). However, no difference was observed between mucilage samples from plants at 60 DAE vs. 90 DAE **(Supplementary Table 1)**. The mucilage fungal microbiome structure was strongly influenced by year of collection (PERMANOVA R-squared= 0.51, $p < 0.001$). Fungal community structure was weakly influenced by developmental stage (PERMANOVA R-squared= 0.02, $p < 0.05$), but not by fertilization status (PERMANOVA, $p > 0.05$) **(Figure 2C).**

The mucilage fungal microbiome was dominated by the Ascomycota (76%) and Basidiomycota (23.7%) phyla. The Dothideomycetes (50%), Sordariomycetes (24%), and Tremellomycetes (14%) fungal classes were the most abundant. Cladosporium (22%), Nectriaceae (17%), Didymellaceae (14%), Bulleribasidiaceae (9 %), Pleosporaceae (8%) were the dominant fungal families in the mucilage. The genera *Cladosporium* exhibited higher abundance in the 2020 growing season (34%) compared with 2021 (14%). In contrast, we found an enrichment of the genera *Epicoccum* in 2021 (18%) compared with the 2020 growing season (0.02%) **(Supplementary Figure 1)**. Taking these results together, Hypothesis 4 was not supported because the bacterial microbiome of mucilage was more sensitive to plant development and consistent across sampling years than the fungal, while the fungal microbiome also exhibited greater variability between years.

Cultivation-dependent bacterial taxonomic and phenotypic diversity of sorghum phyllosphere wax and mucilage.

Bacterial culture collections from the epicuticular wax and aerial root mucilage were constructed by enriching bacteria with putative plant-beneficial traits **(Table 1)**. In total, 500 bacteria from the wax and 800 bacteria from the mucilage were isolated, and then a subset of 200 isolates from both the wax and mucilage were taxonomically identified by sequencing the full-length 16S rRNA gene (**Supplementary Table 2**). These isolates were chosen to represent the range of different cultivation conditions employed and, additionally, to maximize distinguishing phenotypes (morphology, color, etc) to avoid redundancy in the collection (**Figure 5**). The wax bacterial collection was dominated by the Proteobacteria, followed by Actinobacteria, and Bacteroidetes phyla, and the mucilage bacterial collection was dominated by the Proteobacteria, followed by Actinobacteria, Firmicutes, and Bacteroidetes phyla **(Supplementary Table 2)**.

Forty-eight ASVs matched with 100% sequence identity to strains in the isolate collections **(Supplementary Table 2)**. Most of the bacterial families found in the sorghum wax and mucilage had representatives among the isolate collection **(Figure 6)**. Families such as Beijerincklaceae, Chitinophagaceae, Oxalobacteraceae were not captured by our wax bacterial cultivation efforts. Families observed using cultivation-independent techniques but that were not captured by our mucilage cultivation efforts included Cytophagaceae and Oxalobacteraceae.

To understand potential novelty and redundancy represented by the diversity of our wax and mucilage bacterial collections, we compared the full-length 16S rRNA

503 genes with those extracted from the bacterial genomes of previously described non-
504 root-associated, plant-associated (PA) bacteria (Levy et al. 2017), assigned as non-
505 root-associated. 637 bacterial genomes were retrieved from a publicly available
506 database **(**see Methods**)** to provide a reference of context for our 200 sorghum
507 phyllosphere isolates. The final data set contained 527 non-redundant full-length 16S
508 rRNA sequences: 94 new 16S rRNA genes from our sorghum wax and mucilage
509 collections, and 433 rRNA genes from the published plant-associated bacterial
510 genomes (**Figure 7**).
511

512 **DISCUSSION**

513 We investigated the microbiota associated with bioenergy sorghum phyllosphere
514 exudates, specifically from epicuticular wax on stems and leaves and from mucilage on
515 aerial roots.

516 The chemistry of epicuticular wax that covers sorghum stems has been
517 extensively characterized (Bianchi et al. 1978; Jordan et al. 1984; Jenks et al. 2000;
518 Farber et al. 2019a, 2019b), but there is still much to learn about its microbial residents
519 and their colonization dynamics. Thus, we decided to characterize the wax microbiota
520 from stems of field-grown bioenergy sorghum plants at 60 DAE and 90 DAE. We chose
521 these two-time points because they represent different developmental stages, and, in
522 our field conditions, they also had different water availability. During the vegetative
523 stage, sorghum plants at 60 DAE have all leaves developed and fully expanded. At 90
524 DAE in the upper mid-west, plants have transitioned to the reproductive stage, seed

development is in progress and nutrients are being relocated to the kernel. In the southwestern U.S., sorghum plants are in extended vegetative growth stage, with floral initiation expected at 120 DAE. The major lineages we detected in the epicuticular stem wax, including *Proteobacteria*, *Bacteroidetes*, and *Actinobacteria,* agree generally with reports from *Arabidopsis thaliana* and *Sorghum bicolor* epicuticular leaf wax (Reisberg et al. 2013; Sun et al. 2021). Furthermore, we also observed changes in the relative abundances of several taxa at 60 DAE compared with plants at 90 DAE, which could be associated with changes in the composition of the epicuticular wax as the plant grows (Avato et al. 1984; Jenks et al. 1996), though more work is needed to characterize changes in the chemical composition of the wax alongside the structural changes in the microbiome to understand their relationship more fully. It has been suggested that microbes in wax may be able to metabolize wax components and use them as a carbon source (Ueda et al. 2015). Our study enriched several bacterial isolates that were able to grow with linalool and beta-caryophyllene, two of the terpenes found in sorghum wax. To gain further insight into epicuticular wax microbiome assembly and dynamics, next steps could expand this research not only by including samples from different growing seasons, but also by including sorghum genotypes that are mutants in wax production (Jenks et al. 1994, 2000; Peters et al. 2009; Punnuri et al. 2017).

For decades it has been suggested that the sorghum aerial root mucilage harbors diazotroph bacteria (Wani 1986; Bennett et al. 2020). We hypothesized that fertilization would strongly influence the phyllosphere mucilage microbiota due to changes in exogenous nutrient availability and changes in mucilage polysaccharide

547 composition. However, our cultivation-independent data (16S rRNA amplicons) suggest
548 that that differences in nitrogen fertilization had no notable influence on the microbiome
549 structure for both bacterial and fungal communities. In contrast, plant developmental
550 stage strongly affected the mucilage bacterial microbiome structure. Similar evidence of
551 microbiome seasonality has been found in other studies of different surfaces of the
552 phyllosphere microbiome (Copeland et al. 2015; Grady et al. 2019; Xiong et al. 2021;
553 Smets et al. 2022). We also observed several putative diazotroph bacteria in the
554 sorghum mucilage that were isolated anaerobically and on nitrogen-free media,
555 including *Curtobacterium*, *Pantoea, Pseudomonas, Strenotrophomonas*, which were
556 reported as lineages that could colonize the maize mucilage (van Deynze et al. 2018;
557 Higdon et al. 2020b, 2020a).

558 Regarding the fungal microbiome in the mucilage, we found that the year of
559 collection had the highest explanatory value. With two years of field data, there is not
560 enough information to understand if the fungal community is responsive to other
561 covariates (e.g., weather) or more stochastically assembled every year. Fungal
562 community members likely have different responses than bacterial members to
563 changing environmental conditions, including temperature, moisture, solar radiation,
564 and precipitation (Jackson and Denney 2011; Copeland et al. 2015; Wagner et al. 2016;
565 Gomes et al. 2018). We can deduce that the bacterial and fungal communities did not
566 have strong relationships or co-dependencies based on their structures, and likely have
567 different dominating drivers. However, the possibility of redundant functional

568 relationships between different bacterial and fungal mucilage members cannot be
569 eliminated.

570 We combined both culture-independent and dependent approaches to improve
571 our understanding of the microbiome diversity in phyllosphere exudates. Due to the
572 chemical composition, plant DNA contamination, and low bacterial biomass associated
573 with the wax and mucilage, a metagenomic sequencing approach would have been
574 challenging to pursue with the sorghum phyllosphere (Sharpton 2014; van Deynze et al.
575 2018). Sequencing the V4 16S rRNA and the ITS1 regions allowed us to deeply
576 characterize bacterial and fungal communities in sorghum phyllosphere exudates, albeit
577 with limited taxonomic resolution that can be provided by the amplicons (to
578 approximately the genus level Poretsky et al. 2014) as well as limited functional insight
579 (Langille et al. 2013; Turner et al. 2013). Thus, we decided to culture wax and mucilage
580 bacteria by using a variety of isolation media and growing conditions that we expected
581 to enrich for plant-beneficial bacterial phenotypes. In the end, we were able to capture
582 representatives of most of the bacterial families and genera that we observed in our
583 culture-independent approach. These isolates can now be used to test directly for plant
584 beneficial properties and microbe-plant interactions in the laboratory.

585 In summary, we report a characterization of microbiome structure of energy
586 sorghum phyllosphere exudates, epicuticular wax and aerial root mucilage under
587 multiple field conditions and across two seasons for mucilage. We found that the wax
588 and mucilage harbor distinct bacterial communities, suggesting niche specialization in
589 the sorghum phyllosphere, and captured several key bacterial lineages in a parallel

590 cultivation effort. Additionally, we found that fungal communities and bacterial
591 communities in the mucilage are responsive to different drivers, with bacterial
592 communities most distinctive by developmental stage and fungal communities most
593 distinctive by year of sample collection. Next steps are to use the ecological dynamics
594 from the cultivation-independent sequencing and apparent phenotypes of the bacterial
595 isolates to understand the roles of these exudate microbiome members for plant
596 performance.
597

598 **ACKNOWLEDGMENTS**

599 This work was supported by the Great Lakes Bioenergy Research Center, U.S.
600 Department of Energy, Office of Science, Office of Biological and Environmental
601 Research under Award Number DE-SC0018409. Support for field research was
602 provided by the Great Lakes Bioenergy Research Center, U.S. Department of Energy,
603 Office of Science, Office of Biological and Environmental Research (Awards DE-
604 SC0018409 and DE-FC02-07ER64494), by the National Science Foundation Long-term
605 Ecological Research Program (DEB 1637653) at the Kellogg Biological Station, and by
606 Michigan State University AgBioResearch. JM acknowledges field support from
607 graduate students at TAMU. AS acknowledges support from Michigan State University
608 AgBioResearch.
609

610 The authors declare no conflict of interest.
611

612 **LITERATURE CITED**

613 Amicucci, M. J., Galermo, A. G., Guerrero, A., Treves, G., Nandita, E., Kailemia, M. J.,
614 et al. 2019. Strategy for Structural Elucidation of Polysaccharides: Elucidation of
615 a Maize Mucilage that Harbors Diazotrophic Bacteria. Anal Chem. 91:7254–7265
616 Available at: https://doi.org/10.1021/acs.analchem.9b00789.
617 Avato, P., Bianchi, G., and Mariani, G. 1984. Epicuticular waxes of Sorghum and some
618 compositional changes with plant age. Phytochemistry. 23:2843–2846 Available
619 at: https://www.sciencedirect.com/science/article/pii/0031942284830265.
620 Beattie, G. A., and Marcell, L. M. 2002. Effect of alterations in cuticular wax biosynthesis
621 on the physicochemical properties and topography of maize leaf surfaces. Plant
622 Cell Environ. 25:1–16.
623 Bennett, A. B., Pankievicz, V. C. S., and Ané, J.-M. 2020. A Model for Nitrogen Fixation
624 in Cereal Crops. Trends Plant Sci. 25:226–235 Available at:
625 https://www.sciencedirect.com/science/article/pii/S1360138519303292.
626 Bianchi, G., Avato, P., Bertorelli, P., and Mariani, G. 1978. Epicuticular waxes of two
627 sorghum varieties. Phytochemistry. 17:999–1001 Available at:
628 https://www.sciencedirect.com/science/article/pii/S0031942200886689.
629 Bolyen, E., Rideout, J. R., Dillon, M. R., Bokulich, N. A., Abnet, C. C., Al-Ghalith, G. A.,
630 et al. 2019. Reproducible, interactive, scalable and extensible microbiome data
631 science using QIIME 2. Nat Biotechnol. 37:852–857 Available at:
632 https://doi.org/10.1038/s41587-019-0209-9.
633 Bondada, B. R., Oosterhuis, D. M., Murphy, J. B., and Kim, K. S. 1996. Effect of water
634 stress on the epicuticular wax composition and ultrastructure of cotton
635 (Gossypium hirsutum L.) leaf, bract, and boll. Environ Exp Bot. 36:61–69
636 Available at:
637 https://www.sciencedirect.com/science/article/pii/0098847296001281.
638 Busta, L., Schmitz, E., Kosma, D. K., Schnable, J. C., and Cahoon, E. B. 2021. A co-
639 opted steroid synthesis gene, maintained in sorghum but not maize, is
640 associated with a divergence in leaf wax chemistry. Proceedings of the National
641 Academy of Sciences. 118:e2022982118 Available at:
642 https://doi.org/10.1073/pnas.2022982118.
643 Callahan, B. J., McMurdie, P. J., Rosen, M. J., Han, A. W., Johnson, A. J. A., and
644 Holmes, S. P. 2016. DADA2: High-resolution sample inference from Illumina
645 amplicon data. Nat Methods. 13:581–583 Available at:
646 https://doi.org/10.1038/nmeth.3869.
647 Capella-Gutiérrez, S., Silla-Martínez, J. M., and Gabaldón, T. 2009. trimAl: a tool for
648 automated alignment trimming in large-scale phylogenetic analyses.
649 Bioinformatics. 25:1972–1973 Available at:
650 https://doi.org/10.1093/bioinformatics/btp348.
651 Caporaso, G. J., Lauber, C. L., Walters, W., Berg-Lyons, D., Lozupone, C. A.,
652 Turnbaugh, P.J., et al. 2011. Global patterns of 16S rRNA diversity at a depth of
653 millions of sequences per sample. Proceedings of the National Academy of

Sciences. 108:4516–4522 Available at: https://doi.org/10.1073/pnas.1000080107.
Chai, Y. N., and Schachtman, D. P. 2022. Root exudates impact plant performance under abiotic stress. Trends Plant Sci. 27:80–91 Available at: https://doi.org/10.1016/j.tplants.2021.08.003.
Copeland, J. K., Yuan, L., Layeghifard, M., Wang, P. W., and Guttman, D. S. 2015. Seasonal Community Succession of the Phyllosphere Microbiome. Molecular Plant-Microbe Interactions®. 28:274–285 Available at: https://doi.org/10.1094/MPMI-10-14-0331-FI.
van Deynze, A., Zamora, P., Delaux, P.-M., Heitmann, C., Jayaraman, D., Rajasekar, S., et al. 2018. Nitrogen fixation in a landrace of maize is supported by a mucilage-associated diazotrophic microbiota. PLoS Biol. 16:e2006352- Available at: https://doi.org/10.1371/journal.pbio.2006352.
Dixon, P. 2003. VEGAN, A Package of R Functions for Community Ecology. Journal of Vegetation Science. 14:927–930 Available at: http://www.jstor.org/stable/3236992.
Doan, H. K., Ngassam, V. N., Gilmore, S. F., Tecon, R., Parikh, A. N., and Leveau, J. H. J. 2020. Topography-Driven Shape, Spread, and Retention of Leaf Surface Water Impacts Microbial Dispersion and Activity in the Phyllosphere. Phytobiomes J. 4:268–280 Available at: https://doi.org/10.1094/PBIOMES-01-20-0006-R.
Farber, C., Li, J., Hager, E., Chemelewski, R., Mullet, J., Rogachev, A. Y., et al. 2019a. Complementarity of Raman and Infrared Spectroscopy for Structural Characterization of Plant Epicuticular Waxes. ACS Omega. 4:3700–3707 Available at: https://doi.org/10.1021/acsomega.8b03675.
Farber, C., Wang, R., Chemelewski, R., Mullet, J., and Kurouski, D. 2019b. Nanoscale Structural Organization of Plant Epicuticular Wax Probed by Atomic Force Microscope Infrared Spectroscopy. Anal Chem. 91:2472–2479 Available at: https://doi.org/10.1021/acs.analchem.8b05294.
Galloway, A. F., Knox, P., and Krause, K. 2020. Sticky mucilages and exudates of plants: putative microenvironmental design elements with biotechnological value. New Phytologist. 225:1461–1469 Available at: https://doi.org/10.1111/nph.16144.
Gomes, T., Pereira, J. A., Benhadi, J., Lino-Neto, T., and Baptista, P. 2018. Endophytic and Epiphytic Phyllosphere Fungal Communities Are Shaped by Different Environmental Factors in a Mediterranean Ecosystem. Microb Ecol. 76:668–679 Available at: https://doi.org/10.1007/s00248-018-1161-9.
Grady, K. L., Sorensen, J. W., Stopnisek, N., Guittar, J., and Shade, A. 2019. Assembly and seasonality of core phyllosphere microbiota on perennial biofuel crops. Nat Commun. 10:4135 Available at: https://doi.org/10.1038/s41467-019-11974-4.
Higdon, S. M., Pozzo, T., Kong, N., Huang, B. C., Yang, M. L., Jeannotte, R., et al. 2020a. Genomic characterization of a diazotrophic microbiota associated with maize aerial root mucilage. PLoS One. 15:e0239677- Available at: https://doi.org/10.1371/journal.pone.0239677.

Higdon, S. M., Pozzo, T., Tibbett, E. J., Chiu, C., Jeannotte, R., Weimer, B. C., et al. 2020b. Diazotrophic bacteria from maize exhibit multifaceted plant growth promotion traits in multiple hosts. PLoS One. 15:e0239081- Available at: https://doi.org/10.1371/journal.pone.0239081.

Hoang, D. T., Chernomor, O., von Haeseler, A., Minh, B. Q., and Vinh, L. S. 2018. UFBoot2: Improving the Ultrafast Bootstrap Approximation. Mol Biol Evol. 35:518–522 Available at: https://doi.org/10.1093/molbev/msx281.

Jackson, C. R., and Denney, W. C. 2011. Annual and Seasonal Variation in the Phyllosphere Bacterial Community Associated with Leaves of the Southern Magnolia (Magnolia grandiflora). Microb Ecol. 61:113–122 Available at: https://doi.org/10.1007/s00248-010-9742-2.

Jenks, M. A., Joly, R. J., Peters, P. J., Rich, P. J., Axtell, J. D., and Ashworth, E. N. 1994. Chemically Induced Cuticle Mutation Affecting Epidermal Conductance to Water Vapor and Disease Susceptibility in Sorghum bicolor (L.) Moench. Plant Physiol. 105:1239–1245 Available at: https://pubmed.ncbi.nlm.nih.gov/12232280.

Jenks, M. A., Rich, P. J., Rhodes, D., Ashworth, E. N., Axtell, J. D., and Ding, C.-K. 2000. Leaf sheath cuticular waxes on bloomless and sparse-bloom mutants of Sorghum bicolor. Phytochemistry. 54:577–584 Available at: https://www.sciencedirect.com/science/article/pii/S0031942200001539.

Jenks, M. A., Tuttle, H. A., and Feldmann, K. A. 1996. Changes in epicuticular waxes on wildtype and eceriferum mutants in Arabidopsis during development. Phytochemistry. 42:29–34 Available at: https://www.sciencedirect.com/science/article/pii/0031942295008985.

Jordan, W. R., Shouse, P. J., Blum, A., Miller, F. R., and Monk, R. L. 1984. Environmental Physiology of Sorghum. II. Epicuticular Wax Load and Cuticular Transpiration1. Crop Sci. 24:cropsci1984.0011183X002400060038x Available at: https://doi.org/10.2135/cropsci1984.0011183X002400060038x.

Kalyaanamoorthy, S., Minh, B. Q., Wong, T. K. F., von Haeseler, A., and Jermiin, L. S. 2017. ModelFinder: fast model selection for accurate phylogenetic estimates. Nat Methods. 14:587–589 Available at: https://pubmed.ncbi.nlm.nih.gov/28481363.

Katoh, K., Misawa, K., Kuma, K., and Miyata, T. 2002. MAFFT: a novel method for rapid multiple sequence alignment based on fast Fourier transform. Nucleic Acids Res. 30:3059–3066 Available at: https://doi.org/10.1093/nar/gkf436.

Kent, J., Hartman, M. D., Lee, D. K., and Hudiburg, T. 2020. Simulated Biomass Sorghum GHG Reduction Potential is Similar to Maize. Environ Sci Technol. 54:12456–12466 Available at: https://doi.org/10.1021/acs.est.0c01676.

Ku, L. X., Sun, Z. H., Wang, C. L., Zhang, J., Zhao, R. F., Liu, H. Y., et al. 2012. QTL mapping and epistasis analysis of brace root traits in maize. Molecular Breeding. 30:697–708 Available at: https://doi.org/10.1007/s11032-011-9655-x.

Kunst, L., and Samuels, A. L. 2003. Biosynthesis and secretion of plant cuticular wax. Prog Lipid Res. 42:51–80 Available at: https://www.sciencedirect.com/science/article/pii/S0163782702000450.

Langille, M. G. I., Zaneveld, J., Caporaso, J. G., McDonald, D., Knights, D., Reyes, J. A., et al. 2013. Predictive functional profiling of microbial communities using 16S

741 rRNA marker gene sequences. Nat Biotechnol. 31:814–821 Available at:
742 https://doi.org/10.1038/nbt.2676.
743 Letunic, I., and Bork, P. 2021. Interactive Tree Of Life (iTOL) v5: an online tool for
744 phylogenetic tree display and annotation. Nucleic Acids Res. 49:W293–W296
745 Available at: https://doi.org/10.1093/nar/gkab301.
746 Levy, A., Salas Gonzalez, I., Mittelviefhaus, M., Clingenpeel, S., Herrera Paredes, S.,
747 Miao, J., et al. 2017. Genomic features of bacterial adaptation to plants. Nat
748 Genet. 50:138–150 Available at: https://pubmed.ncbi.nlm.nih.gov/29255260.
749 Li, W., and Godzik, A. 2006. Cd-hit: a fast program for clustering and comparing large
750 sets of protein or nucleotide sequences. Bioinformatics. 22:1658–1659 Available
751 at: https://doi.org/10.1093/bioinformatics/btl158.
752 Lindow, S. E., and Brandl, M. T. 2003. Microbiology of the phyllosphere. Appl Environ
753 Microbiol. 69:1875–1883 Available at:
754 https://pubmed.ncbi.nlm.nih.gov/12676659.
755 Love, M. I., Huber, W., and Anders, S. 2014. Moderated estimation of fold change and
756 dispersion for RNA-seq data with DESeq2. Genome Biol. 15:550 Available at:
757 https://doi.org/10.1186/s13059-014-0550-8.
758 McMurdie, P. J., and Holmes, S. 2013. phyloseq: An R Package for Reproducible
759 Interactive Analysis and Graphics of Microbiome Census Data. PLoS One.
760 8:e61217- Available at: https://doi.org/10.1371/journal.pone.0061217.
761 Miller, C. S., Handley, K. M., Wrighton, K. C., Frischkorn, K. R., Thomas, B. C., and
762 Banfield, J. F. 2013. Short-Read Assembly of Full-Length 16S Amplicons
763 Reveals Bacterial Diversity in Subsurface Sediments. PLoS One. 8:e56018-
764 Available at: https://doi.org/10.1371/journal.pone.0056018.
765 Minh, B. Q., Schmidt, H. A., Chernomor, O., Schrempf, D., Woodhams, M. D., von
766 Haeseler, A., et al. 2020. IQ-TREE 2: New Models and Efficient Methods for
767 Phylogenetic Inference in the Genomic Era. Mol Biol Evol. 37:1530–1534
768 Available at: https://doi.org/10.1093/molbev/msaa015.
769 Mullet, J., Morishige, D., McCormick, R., Truong, S., Hilley, J., McKinley, B., et al. 2014.
770 Energy Sorghum—a genetic model for the design of C4 grass bioenergy crops. J
771 Exp Bot. 65:3479–3489 Available at: https://doi.org/10.1093/jxb/eru229.
772 Nazari, M., Riebeling, S., Banfield, C. C., Akale, A., Crosta, M., Mason-Jones, K., et al.
773 2020. Mucilage Polysaccharide Composition and Exudation in Maize From
774 Contrasting Climatic Regions. Front Plant Sci. 11 Available at:
775 https://www.frontiersin.org/article/10.3389/fpls.2020.587610.
776 Nilsson, R. H., Larsson, K.-H., Taylor, A. F. S., Bengtsson-Palme, J., Jeppesen, T. S.,
777 Schigel, D., et al. 2019. The UNITE database for molecular identification of fungi:
778 handling dark taxa and parallel taxonomic classifications. Nucleic Acids Res.
779 47:D259–D264 Available at: https://doi.org/10.1093/nar/gky1022.
780 Olson, S. N., Ritter, K., Rooney, W., Kemanian, A., McCarl, B. A., Zhang, Y., et al.
781 2012. High biomass yield energy sorghum: developing a genetic model for C4
782 grass bioenergy crops. Biofuels, Bioproducts and Biorefining. 6:640–655
783 Available at: https://doi.org/10.1002/bbb.1357.

784 Peters, P. J., Jenks, M. A., Rich, P. J., Axtell, J. D., and Ejeta, G. 2009. Mutagenesis,
785 Selection, and Allelic Analysis of Epicuticular Wax Mutants in Sorghum. Crop Sci.
786 49:1250–1258 Available at: https://doi.org/10.2135/cropsci2008.08.0461.
787 Pierce, M. P. 2019. The ecological and evolutionary importance of nectar-secreting
788 galls. Ecosphere. 10:e02670 Available at: https://doi.org/10.1002/ecs2.2670.
789 Poretsky, R., Rodriguez-R, L. M., Luo, C., Tsementzi, D., and Konstantinidis, K. T.
790 2014. Strengths and Limitations of 16S rRNA Gene Amplicon Sequencing in
791 Revealing Temporal Microbial Community Dynamics. PLoS One. 9:e93827-
792 Available at: https://doi.org/10.1371/journal.pone.0093827.
793 Punnuri, S., Harris-Shultz, K., Knoll, J., Ni, X., and Wang, H. 2017. The Genes Bm2 and
794 Blmc that Affect Epicuticular Wax Deposition in Sorghum are Allelic. Crop Sci.
795 57:1552–1556 Available at: https://doi.org/10.2135/cropsci2016.11.0937.
796 Quast, C., Pruesse, E., Yilmaz, P., Gerken, J., Schweer, T., Yarza, P., et al. 2013. The
797 SILVA ribosomal RNA gene database project: improved data processing and
798 web-based tools. Nucleic Acids Res. 41:D590–D596 Available at:
799 https://doi.org/10.1093/nar/gks1219.
800 Reisberg, E. E., Hildebrandt, U., Riederer, M., and Hentschel, U. 2013. Distinct
801 phyllosphere bacterial communities on Arabidopsis wax mutant leaves. PLoS
802 One. 8:e78613–e78613 Available at: https://pubmed.ncbi.nlm.nih.gov/24223831.
803 Reneau, J. W., Khangura, R. S., Stager, A., Erndwein, L., Weldekidan, T., Cook, D. D.,
804 et al. 2020. Maize brace roots provide stalk anchorage. Plant Direct. 4:e00284
805 Available at: https://doi.org/10.1002/pld3.284.
806 Rering, C. C., Beck, J. J., Hall, G. W., McCartney, M. M., and Vannette, R. L. 2018.
807 Nectar-inhabiting microorganisms influence nectar volatile composition and
808 attractiveness to a generalist pollinator. New Phytologist. 220:750–759 Available
809 at: https://doi.org/10.1111/nph.14809.
810 Ruinen, J. 1965. The phyllosphere. Plant Soil. 22:375–394 Available at:
811 https://doi.org/10.1007/BF01422435.
812 Scully, M. J., Norris, G. A., Alarcon Falconi, T. M., and MacIntosh, D. L. 2021. Carbon
813 intensity of corn ethanol in the United States: state of the science. Environmental
814 Research Letters. 16:043001 Available at: http://dx.doi.org/10.1088/1748-
815 9326/abde08.
816 Seemann, T. 2014. Prokka: rapid prokaryotic genome annotation. Bioinformatics.
817 30:2068–2069 Available at: https://doi.org/10.1093/bioinformatics/btu153.
818 Serrano, M., Coluccia, F., Torres, M., L'Haridon, F., and Métraux, J.-P. 2014. The
819 cuticle and plant defense to pathogens. Front Plant Sci. 5:274 Available at:
820 https://pubmed.ncbi.nlm.nih.gov/24982666.
821 Sharpton, T. J. 2014. An introduction to the analysis of shotgun metagenomic data.
822 Front Plant Sci. 5 Available at:
823 https://www.frontiersin.org/article/10.3389/fpls.2014.00209.
824 Shepherd, T., Robertson, G. W., Griffiths, D. W., Birch, A. N. E., and Duncan, G. 1995.
825 Effects of environment on the composition of epicuticular wax from kale and
826 swede. Phytochemistry. 40:407–417 Available at:
827 https://www.sciencedirect.com/science/article/pii/003194229500281B.

Shepherd, T., and Wynne Griffiths, D. 2006. The effects of stress on plant cuticular waxes. New Phytologist. 171:469–499 Available at: https://doi.org/10.1111/j.1469-8137.2006.01826.x.

Smets, W., Spada, M. L., Gandolfi, I., Wuyts, K., Legein, M., Muyshondt, B., et al. 2022. Bacterial Succession and Community Dynamics of the Emerging Leaf Phyllosphere in Spring. Microbiol Spectr. 10:e02420-21 Available at: https://doi.org/10.1128/spectrum.02420-21.

Stamp, P., and Kiel, C. 1992. Root Morphology of Maize and Its Relationship to Root Lodging. J Agron Crop Sci. 168:113–118 Available at: https://doi.org/10.1111/j.1439-037X.1992.tb00987.x.

Steinmüller, D., and Tevini, M. 1985. Action of ultraviolet radiation (UV-B) upon cuticular waxes in some crop plants. Planta. 164:557–564 Available at: https://doi.org/10.1007/BF00395975.

Sun, A., Jiao, X.-Y., Chen, Q., Wu, A.-L., Zheng, Y., Lin, Y.-X., et al. 2021. Microbial communities in crop phyllosphere and root endosphere are more resistant than soil microbiota to fertilization. Soil Biol Biochem. 153:108113 Available at: https://www.sciencedirect.com/science/article/pii/S0038071720304090.

Tsuba, M., Katagiri, C., Takeuchi, Y., Takada, Y., and Yamaoka, N. 2002. Chemical factors of the leaf surface involved in the morphogenesis of Blumeria graminis. Physiol Mol Plant Pathol. 60:51–57 Available at: https://www.sciencedirect.com/science/article/pii/S0885576502903760.

Turner, T. R., James, E. K., and Poole, P. S. 2013. The plant microbiome. Genome Biol. 14:209 Available at: https://doi.org/10.1186/gb-2013-14-6-209.

Ueda, H., Mitsuhara, I., Tabata, J., Kugimiya, S., Watanabe, T., Suzuki, K., et al. 2015. Extracellular esterases of phylloplane yeast Pseudozyma antarctica induce defect on cuticle layer structure and water-holding ability of plant leaves. Appl Microbiol Biotechnol. 99:6405–6415 Available at: https://doi.org/10.1007/s00253-015-6523-3.

Vacher, C., Hampe, A., Porté, A. J., Sauer, U., Compant, S., and Morris, C. E. 2016. The Phyllosphere: Microbial Jungle at the Plant–Climate Interface. Annu Rev Ecol Evol Syst. 47:1–24 Available at: https://doi.org/10.1146/annurev-ecolsys-121415-032238.

Varoquaux, N., Cole, B., Gao, C., Pierroz, G., Baker, C. R., Patel, D., et al. 2019. Transcriptomic analysis of field-droughted sorghum from seedling to maturity reveals biotic and metabolic responses. Proceedings of the National Academy of Sciences. 116:27124–27132 Available at: https://doi.org/10.1073/pnas.1907500116.

Vorholt, J. A. 2012. Microbial life in the phyllosphere. Nat Rev Microbiol. 10:828–840 Available at: https://doi.org/10.1038/nrmicro2910.

Wagner, M. R., Lundberg, D. S., del Rio, T. G., Tringe, S. G., Dangl, J. L., and Mitchell-Olds, T. 2016. Host genotype and age shape the leaf and root microbiomes of a wild perennial plant. Nat Commun. 7:12151 Available at: https://doi.org/10.1038/ncomms12151.

Wani, S. 1986. Cereal nitrogen fixation: Proceedings of the Working Group meeting held at ICRISAY Center, India, 9-12 October 1984. Available at: http://oar.icrisat.org/851/

Wang, X., Kong, L., Zhi, P., and Chang, C. 2020. Update on Cuticular Wax Biosynthesis and Its Roles in Plant Disease Resistance. Int J Mol Sci. 21:5514 Available at: https://pubmed.ncbi.nlm.nih.gov/32752176.

Weinstein, M. M., Prem, A., Jin, M., Tang, S., and Bhasin, J. M. 2019. FIGARO: An efficient and objective tool for optimizing microbiome rRNA gene trimming parameters. bioRxiv. :610394 Available at: http://biorxiv.org/content/early/2019/04/16/610394.abstract.

von Wettstein-Knowles, P. 1974. Ultrastructure and origin of epicuticular wax tubes. J Ultrastruct Res. 46:483–498 Available at: https://www.sciencedirect.com/science/article/pii/S0022532074900690.

Xiong, C., Singh, B. K., He, J.-Z., Han, Y.-L., Li, P.-P., Wan, L.-H., et al. 2021. Plant developmental stage drives the differentiation in ecological role of the maize microbiome. Microbiome. 9:171 Available at: https://doi.org/10.1186/s40168-021-01118-6.

Xue, D., Zhang, X., Lu, X., Chen, G., and Chen, Z.-H. 2017. Molecular and Evolutionary Mechanisms of Cuticular Wax for Plant Drought Tolerance. Front Plant Sci. 8:621 Available at: https://pubmed.ncbi.nlm.nih.gov/28503179.

Yeats, T. H., and Rose, J. K. C. 2013. The formation and function of plant cuticles. Plant Physiol. 163:5–20 Available at: https://pubmed.ncbi.nlm.nih.gov/23893170.

895 **TABLES**

896 **Table 1.** Solid media and their enrichment objectives (target phenotypes) used in this
897 study to culture bacteria from the sorghum wax and mucilage. Dilutions from 10^{-1} to 10^{-4}
898 were plated for each condition, for each exudate.

899

Media	Target phenotype	Temperature (°C)	Oxygen condition
Reasoner's 2A agar (R2A)	General diversity	25, 37	Aerobic, anaerobic
50% R2A	General diversity	25, 37	Aerobic, anaerobic
Tryptic Soy Agar (TSA)	General diversity	25, 37	Aerobic, anaerobic
50% TSA	General diversity	25, 37	Aerobic, anaerobic
M9 minimal medium	General diversity	25, 37	Aerobic, anaerobic
King's B medium	*Pseudomonas* species	25, 37	Aerobic, anaerobic
Nitrogen-free Jensen's medium	Nitrogen fixation	25, 37	Aerobic, anaerobic
M9 minimal medium nitrogen-free, 1% xylose	Nitrogen fixation	25, 37	Aerobic, anaerobic
M9 minimal medium nitrogen-free, 1% galactose	Nitrogen fixation	25, 37	Aerobic, anaerobic
M9 minimal medium nitrogen-free, 1% arabinose	Nitrogen fixation	25, 37	Aerobic, anaerobic
M9 minimal medium nitrogen-carbon free	Nitrogen fixation	25, 37	Aerobic, anaerobic
Pirovskaya's agar	Phosphate solubilization	25, 37	Aerobic, anaerobic
50% Tryptic Soy Broth, 1% linalool*	Resistance to/utilization of terpenoids	28	Aerobic
50% Tryptic Soy Broth, 1% β-caryophyllene*	Resistance to/utilization of terpenoids	28	Aerobic
50% Tryptic Soy Broth, 6000 Polyethylene Glycol*	Osmotic tolerance	28	Aerobic
Gauze's synthetic medium N-1	Actinobacteria species	25	Aerobic

Methanol Mineral Salts Medium	Methylotrophs	25	Aerobic

*After initial enrichment in liquid media, turbid cultures were diluted and plated onto R2A to isolate colonies.

903

904 **Table 2.** Sequencing summary of sorghum epicuticular wax and aerial root mucilage

905 microbial communities characterized in this study.

	Wax (16S rRNA) 2020	Mucilage (16S rRNA) 2020	Mucilage (16S rRNA) 2021	Mucilage (ITS1) 2020	Mucilage (ITS1) 2021
Number of samples	48	99	80	92	81
Raw Read Pairs	8,648,839	12,783,054	10,034,885	10,403,184	9,778,220
QC reads	7,930,768	10,809,135	9,071,499	6,200,571	5,957,248
% Chloroplast/ Mitochondria/ unassigned of QC reads	70%	24%	48%	0%	0%

906

907

908

909 **Table 3.** Permuted multivariate analysis of variance (PERMANOVA) to test for

910 microbiome differences in beta diversity.

Dataset	Exudate	Variable tested	Degrees of freedom	Pseudo F	R-squared	*p*-value
Bacteria	Mucilage, wax	Exudate	1	35.51	0.14	<0.001
	Mucilage	Development	1	25.22	0.14	<0.001
	Mucilage	Fertilization	1	4.26	0.03	<0.001
	Mucilage	Year	1	3.36	0.02	<0.001
	Mucilage	Fertilization*Development	1	1.78	0.01	0.05
	Mucilage	Development*Year	1	2.78	0.01	<0.01
	Mucilage	Fertilization*Year	1	1.64	0.01	0.06
	Wax	Development	1	2.75	0.06	<0.01
Fungi	Mucilage	Development	1	3.25	0.02	<0.05
	Mucilage	Fertilization	1	2.20	0.01	0.07
	Mucilage	Year	1	176.38	0.51	<0.001
	Mucilage	Fertilization*Development	1	0.57	0.00	0.68
	Mucilage	Development*Year	1	5.03	0.01	<0.01
	Mucilage	Fertilization*Year	1	4.29	0.01	<0.05

911

912 **Figure Legends**

913 **Figure 1.** Sequencing effort and alpha diversity for sorghum epicuticular wax and aerial
914 root mucilage. Amplicon sequencing variants (ASVs) were defined at 100% identity of
915 16S rRNA gene or ITS1 gene for bacterial and fungal datasets, respectively.
916 Subsampled read depth is indicated by the red, vertical, dashed line. Top panel:
917 Rarefaction curves of quality-controlled sequences. Bottom panels: Observed taxa (No.
918 ASVs, *a.k.a.* richness) and phylogenetic diversity (PD) metrics. A) Epicuticular wax
919 bacterial samples were rarefied to 1,303 reads per sample. B) Aerial root mucilage
920 bacterial samples were rarefied to 20,519 reads per sample. C) Aerial root mucilage
921 fungal samples were rarefied to 33,975 reads per sample.
922
923 **Figure 2.** Relative abundances of bacterial families in sorghum epicuticular wax (A) and
924 aerial root mucilage (B) at 60 and 90 days after plant emergence; and relative
925 abundances of fungal families in mucilage (C) from samples collected in 2020 and
926 2021. Only families with relative abundances >0.03 are shown.
927
928 **Figure 3.** Principal Coordinates Analysis (PCoA) based on Bray-Curtis dissimilarities for
929 bacterial microbiome from sorghum epicuticular wax (A), bacterial microbiome from
930 aerial root mucilage (B) and fungal microbiome from mucilage (C). DAE is days after
931 plant emergence.
932

933 **Figure 4.** Differential abundance analysis for amplicon sequencing variants (ASVs)
934 defined at 100% sequence identity. Differentially enriched bacterial ASVs in the aerial
935 root mucilage of plants at 60 and 90 DAE are shown. The fold change is shown on the
936 x-axis and bacterial genera are listed on the y-axis. Each colored dot represents a
937 separate ASV annotated within a bacterial Class.
938
939 **Figure 5.** Taxonomic diversity of the subset of bacteria cultivated from sorghum
940 epicuticular wax and aerial root mucilage that were selected for 16S rRNA gene
941 sequence analysis based on representation of different cultivation conditions and colony
942 phenotypes. A) Bacterial isolates cultured at 25°C under aerobic conditions, B) Bacterial
943 isolates cultured at 37°C under aerobic conditions, C) Bacterial isolates cultured at 25°C
944 under anaerobic conditions, and D) Bacterial isolates cultured at 37°C under anaerobic
945 conditions.
946
947 **Figure 6.** Overlap in bacterial diversity found in the sorghum epicuticular wax and aerial
948 root mucilage based on culture-independent and culture-dependent approaches.
949 Relative abundance at the family level > 0.01 are shown.
950
951 **Figure 7.** Phylogenetic diversity in the sorghum epicuticular wax and aerial root
952 mucilage. Maximum Likelihood phylogenetic tree (IQTREE, under UNREST+FO+I+G4
953 model) is based on the 16S rRNA gene alignment from nonredundant sorghum bacterial
954 isolates and Levy et al. 2017 genomes.

Supplementary Information

Supplementary Figure S1. Relative abundances of bacterial genera in sorghum epicuticular wax (A) and aerial root mucilage (B) at 60 and 90 days after plant emergence; and relative abundances of fungal families in mucilage (C) from samples collected in 2020 and 2021. Only genera with relative abundances >0.03 are shown.

Supplementary Table S1. *Excel file.* Tests for differences in bacterial and fungal alpha diversity (richness, *a.k.a.* number of observed taxa) between exudates (mucilage, wax) and, within each exudate, between categories of development (60 v. 90 DAE), fertilization (nitrogen-fertilized, unfertilized), and year (2020, 2021) using the Wilcoxon rank sum test with continuity correction.

Supplementary Table S2. *Excel file.* Bacterial isolates from wax and mucilage and their taxonomy based on full-length 16S rRNA gene Sanger sequencing. The isolates that shared 100% sequence identity to short-read bacterial ASVs (Amplicon Sequencing Variants) are indicated and mapped to the ASV ID.

Mechan Llontop, Mullet and Shade
Phyllosphere exudates select for distinct microbiome members in sorghum epicuticular wax and aerial root mucilage
Figure 1

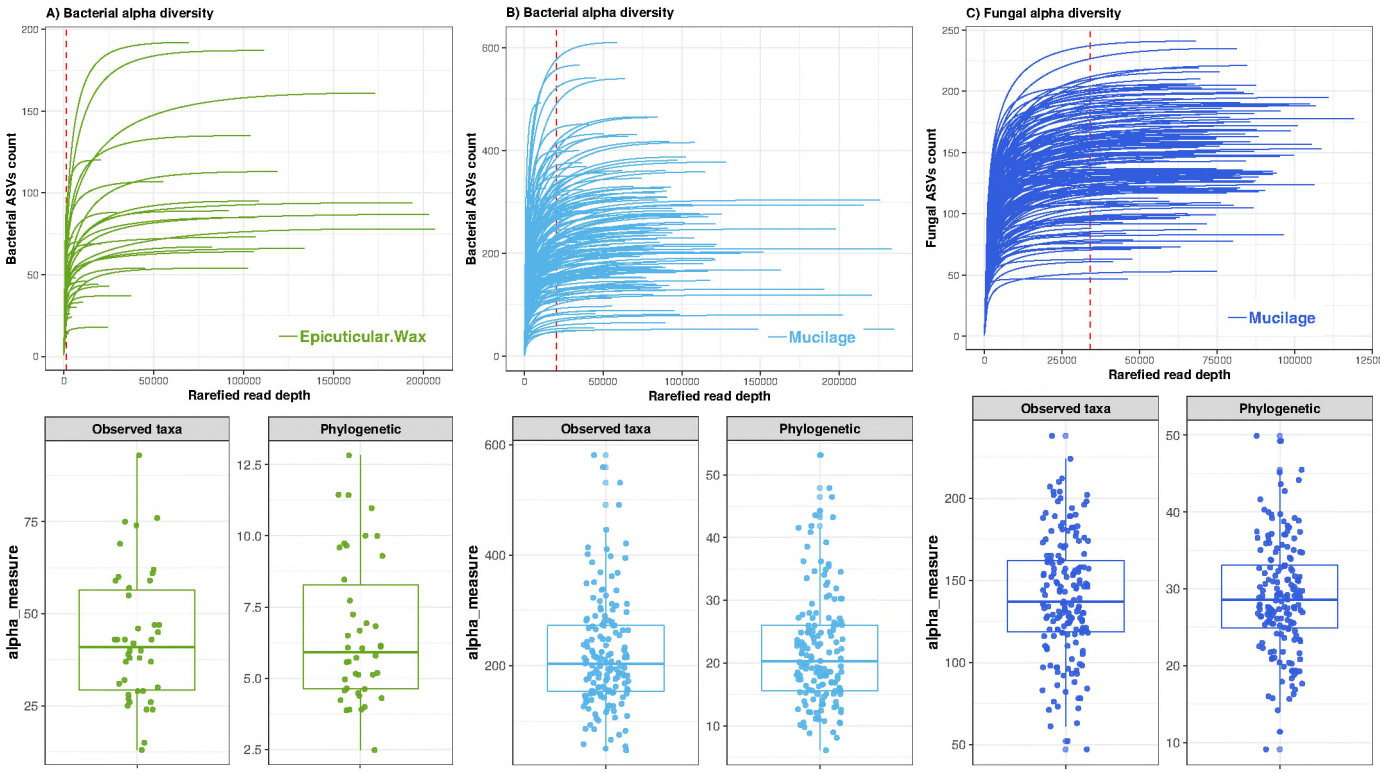

Mechan Llontop, Mullet and Shade
Phyllosphere exudates select for distinct microbiome members in sorghum epicuticular wax and aerial root mucilage
Figure 2

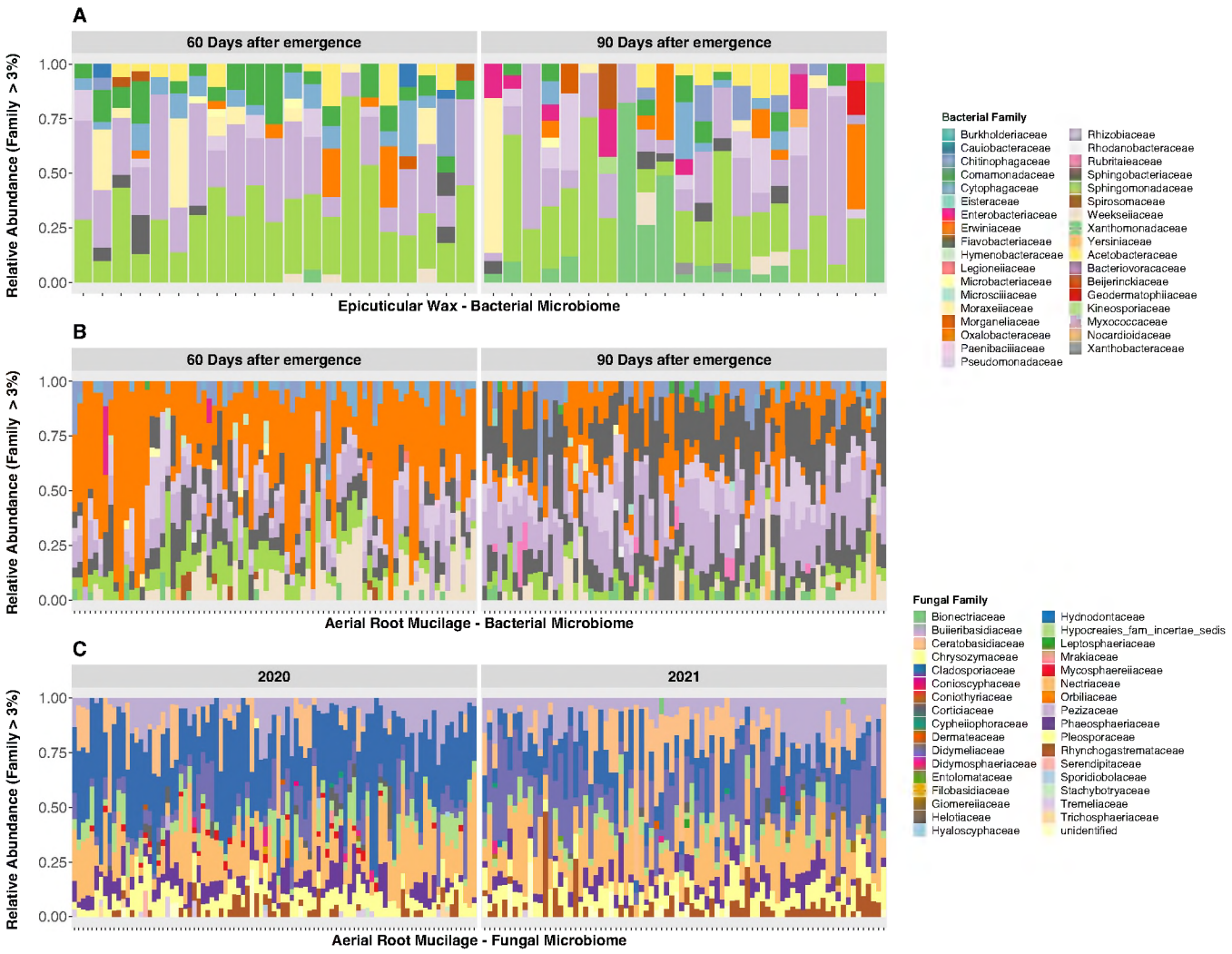

Mechan Llontop, Mullet and Shade
Phyllosphere exudates select for distinct microbiome members in sorghum epicuticular wax and aerial root mucilage
Figure 3

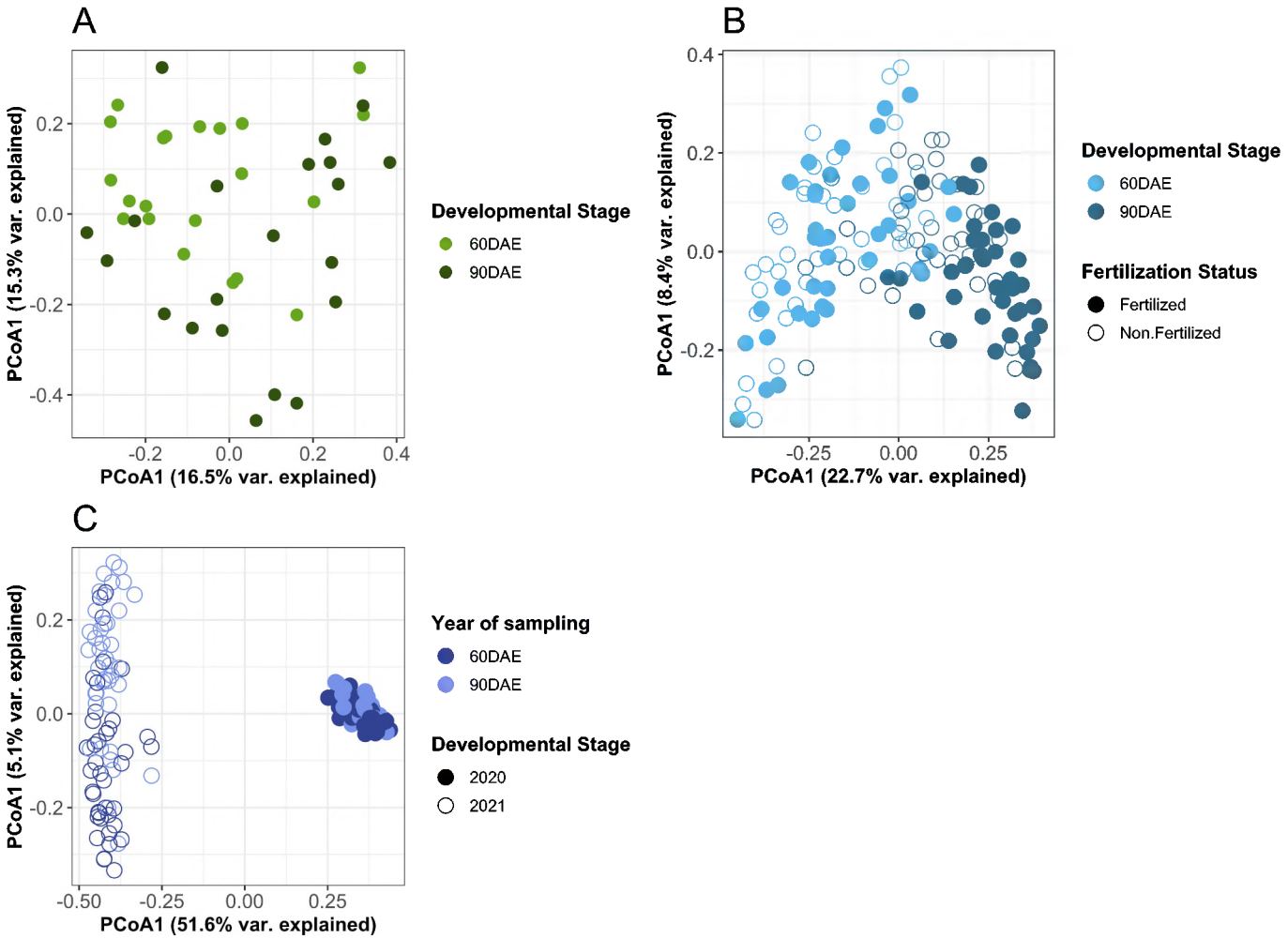

Mechan Llontop, Mullet and Shade
Phyllosphere exudates select for distinct microbiome members in sorghum epicuticular wax and aerial root mucilage
Figure 4

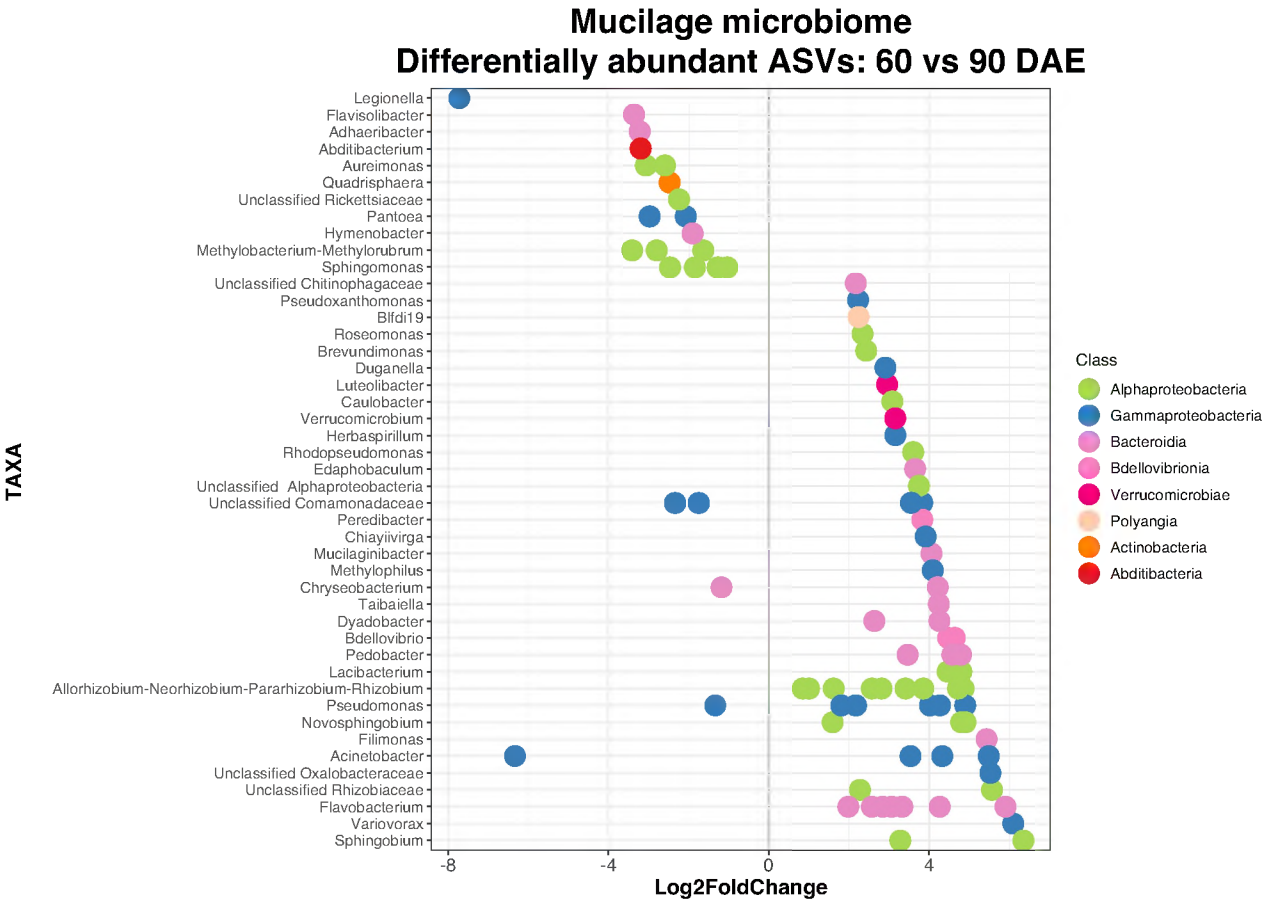

Mechan Llontop, Mullet and Shade
Phyllosphere exudates select for distinct microbiome members in sorghum epicuticular wax and aerial root mucilage
Figure 5

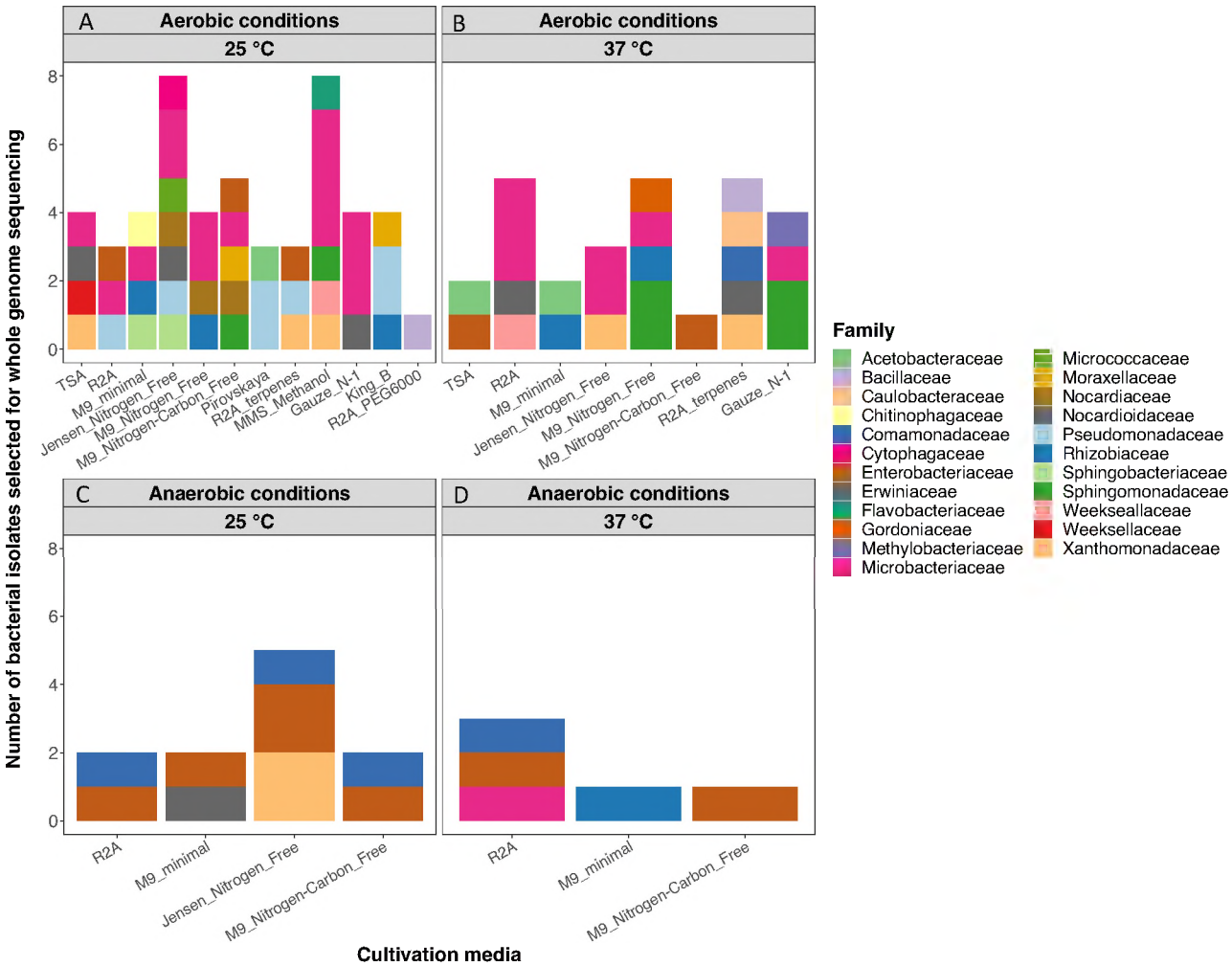

Mechan Llontop, Mullet and Shade
Phyllosphere exudates select for distinct microbiome members in sorghum epicuticular wax and aerial root mucilage
Figure 6

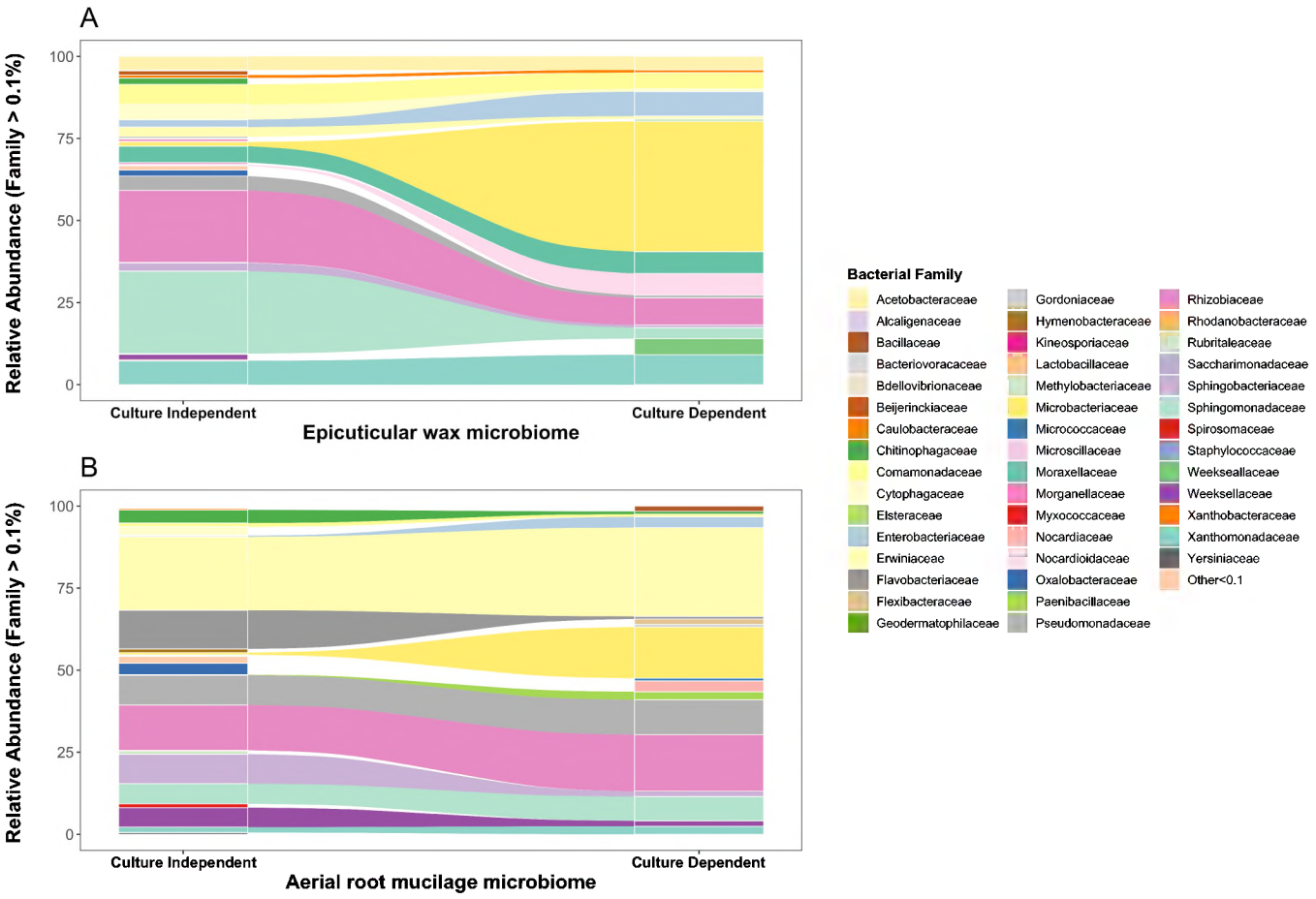

Mechan Llontop, Mullet and Shade
Phyllosphere exudates select for distinct microbiome members in sorghum epicuticular wax and aerial root mucilage
Figure 7

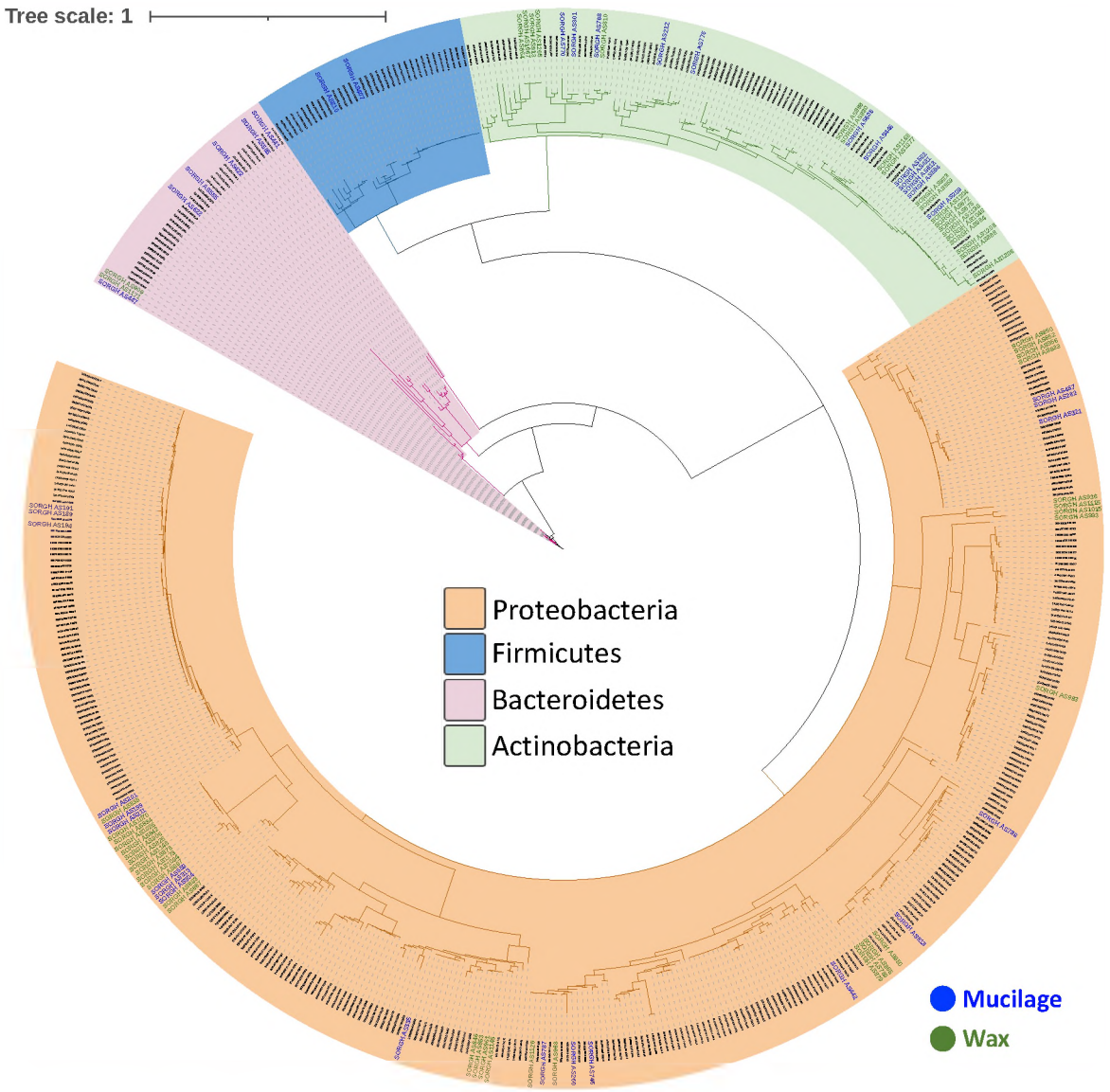

A

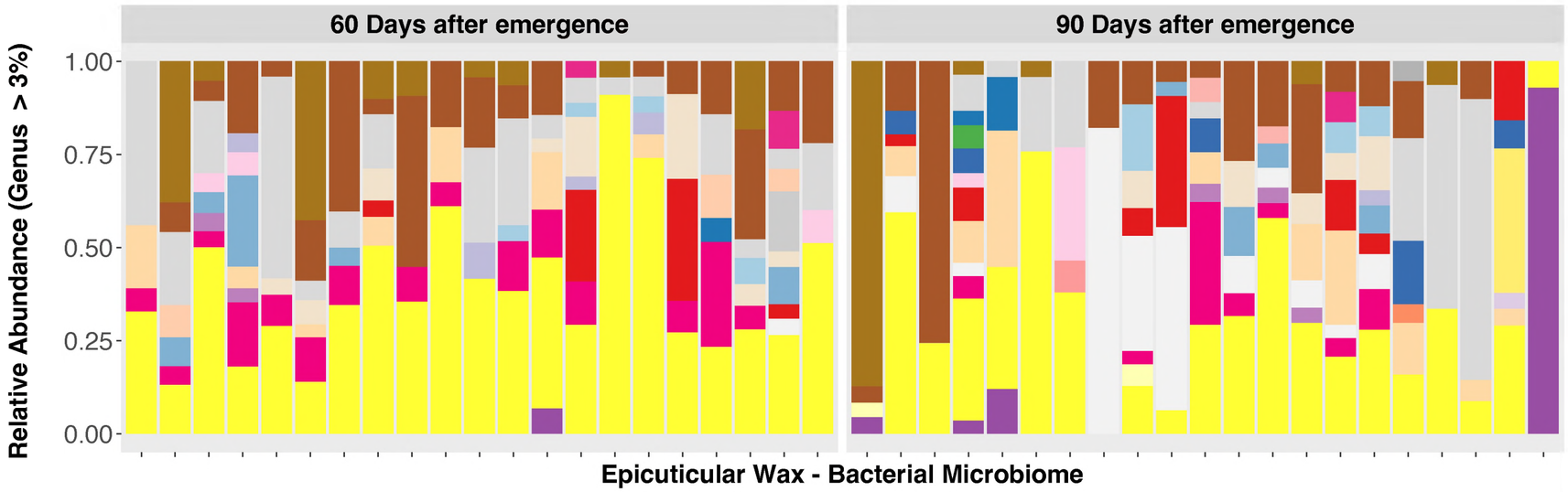
60 Days after emergence
90 Days after emergence
Relative Abundance (Genus > 3%)
1.00
0.75
0.50
0.25
0.00
Epicuticular Wax - Bacterial Microbiome

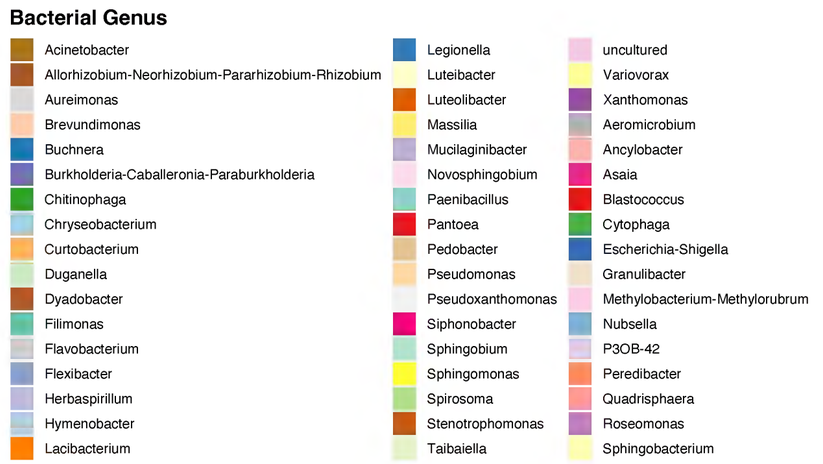
Bacterial Genus
Acinetobacter
Allorhizobium-Neorhizobium-Pararhizobium-Rhizobium
Aureimonas
Brevundimonas
Buchnera
Burkholderia-Caballeronia-Paraburkholderia
Chitinophaga
Chryseobacterium
Curtobacterium
Duganella
Dyadobacter
Filimonas
Flavobacterium
Flexibacter
Herbaspirillum
Hymenobacter
Lacibacterium
Legionella
Luteibacter
Luteolibacter
Massilia
Mucilaginibacter
Novosphingobium
Paenibacillus
Pantoea
Pedobacter
Pseudomonas
Pseudoxanthomonas
Siphonobacter
Sphingobium
Sphingomonas
Spirosoma
Stenotrophomonas
Taibaiella
uncultured
Variovorax
Xanthomonas
Aeromicrobium
Ancylobacter
Asaia
Blastococcus
Cytophaga
Escherichia-Shigella
Granulibacter
Methylobacterium-Methylorubrum
Nubsella
P3OB-42
Peredibacter
Quadrisphaera
Roseomonas
Sphingobacterium

B

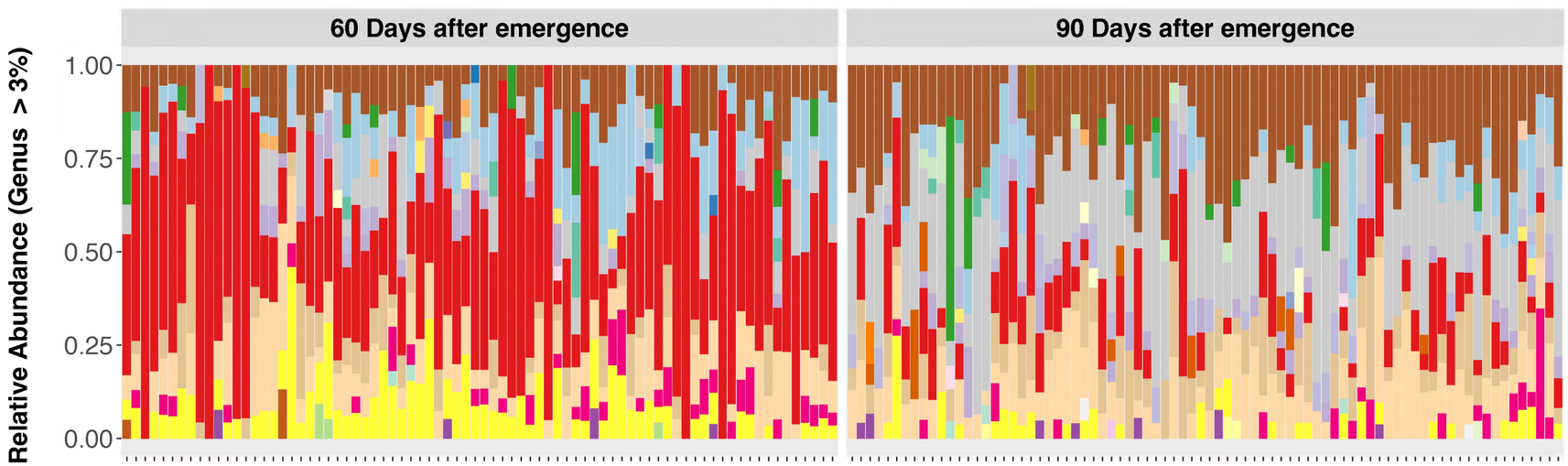
60 Days after emergence
90 Days after emergence
Relative Abundance (Genus > 3%)
1.00
0.75
0.50
0.25
0.00
Aerial Root Mucilage - Bacterial Microbiome

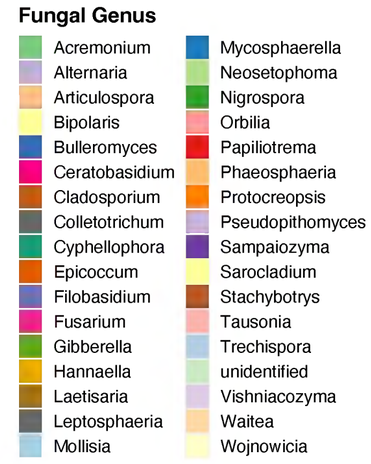
Fungal Genus
Acremonium
Alternaria
Articulospora
Bipolaris
Bulleromyces
Ceratobasidium
Cladosporium
Colletotrichum
Cyphellophora
Epicoccum
Filobasidium
Fusarium
Gibberella
Hannaella
Laetisaria
Leptosphaeria
Mollisia
Mycosphaerella
Neosetophoma
Nigrospora
Orbilia
Papiliotrema
Phaeosphaeria
Protocreopsis
Pseudopithomyces
Sampaiozyma
Sarocladium
Stachybotrys
Tausonia
Trechispora
unidentified
Vishniacozyma
Waitea
Wojnowicia

C

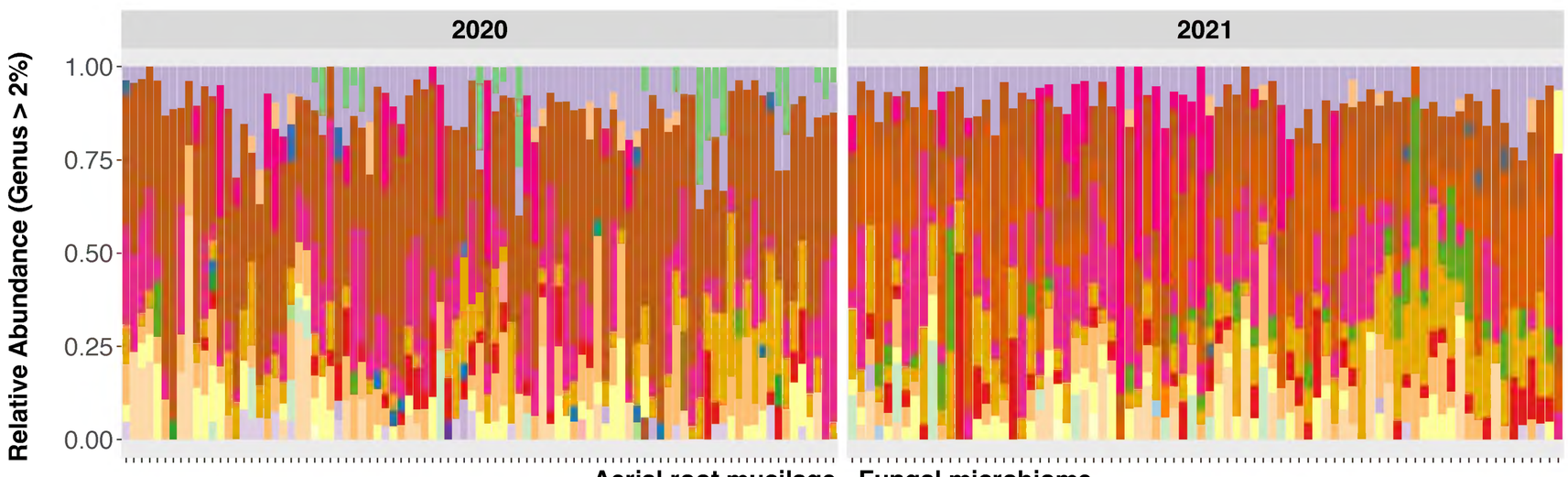
2020
2021
Relative Abundance (Genus > 2%)
1.00
0.75
0.50
0.25
0.00
Aerial root mucilage - Fungal microbiome